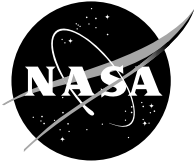


NASA/CR—2004-213311



Study of Vacuum Energy Physics for Breakthrough Propulsion

G. Jordan Maclay
Quantum Fields LLC, Richland Center, Wisconsin

Jay Hammer and Rod Clark
MEMS Optical, Inc., Huntsville, Alabama

Michael George, Yeong Kim, and Asit Kir
University of Alabama, Huntsville, Alabama

The NASA STI Program Office . . . in Profile

Since its founding, NASA has been dedicated to the advancement of aeronautics and space science. The NASA Scientific and Technical Information (STI) Program Office plays a key part in helping NASA maintain this important role.

The NASA STI Program Office is operated by Langley Research Center, the Lead Center for NASA's scientific and technical information. The NASA STI Program Office provides access to the NASA STI Database, the largest collection of aeronautical and space science STI in the world. The Program Office is also NASA's institutional mechanism for disseminating the results of its research and development activities. These results are published by NASA in the NASA STI Report Series, which includes the following report types:

- **TECHNICAL PUBLICATION.** Reports of completed research or a major significant phase of research that present the results of NASA programs and include extensive data or theoretical analysis. Includes compilations of significant scientific and technical data and information deemed to be of continuing reference value. NASA's counterpart of peer-reviewed formal professional papers but has less stringent limitations on manuscript length and extent of graphic presentations.
- **TECHNICAL MEMORANDUM.** Scientific and technical findings that are preliminary or of specialized interest, e.g., quick release reports, working papers, and bibliographies that contain minimal annotation. Does not contain extensive analysis.
- **CONTRACTOR REPORT.** Scientific and technical findings by NASA-sponsored contractors and grantees.

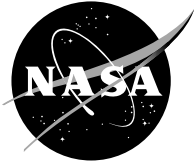
- **CONFERENCE PUBLICATION.** Collected papers from scientific and technical conferences, symposia, seminars, or other meetings sponsored or cosponsored by NASA.
- **SPECIAL PUBLICATION.** Scientific, technical, or historical information from NASA programs, projects, and missions, often concerned with subjects having substantial public interest.
- **TECHNICAL TRANSLATION.** English-language translations of foreign scientific and technical material pertinent to NASA's mission.

Specialized services that complement the STI Program Office's diverse offerings include creating custom thesauri, building customized databases, organizing and publishing research results . . . even providing videos.

For more information about the NASA STI Program Office, see the following:

- Access the NASA STI Program Home Page at <http://www.sti.nasa.gov>
- E-mail your question via the Internet to help@sti.nasa.gov
- Fax your question to the NASA Access Help Desk at 301-621-0134
- Telephone the NASA Access Help Desk at 301-621-0390
- Write to:
NASA Access Help Desk
NASA Center for Aerospace Information
7121 Standard Drive
Hanover, MD 21076

NASA/CR—2004-213311



Study of Vacuum Energy Physics for Breakthrough Propulsion

G. Jordan Maclay
Quantum Fields LLC, Richland Center, Wisconsin

Jay Hammer and Rod Clark
MEMS Optical, Inc., Huntsville, Alabama

Michael George, Yeong Kim, and Asit Kir
University of Alabama, Huntsville, Alabama

Prepared under Contract NAS3-00093

National Aeronautics and
Space Administration

Glenn Research Center

October 2004

This report contains preliminary findings, subject to revision as analysis proceeds.

Trade names or manufacturers' names are used in this report for identification only. This usage does not constitute an official endorsement, either expressed or implied, by the National Aeronautics and Space Administration.

Available from

NASA Center for Aerospace Information
7121 Standard Drive
Hanover, MD 21076

National Technical Information Service
5285 Port Royal Road
Springfield, VA 22100

Available electronically at <http://gltrs.grc.nasa.gov>

CONTENTS

1	Summary	2
2	Development of AFM Instrumentation	6
2.1	Experimental Methods	10
2.1.1	Assembly of Cantilevers	10
2.1.2	Cavity Substrates	10
2.1.3	Electrostatic Calibration	14
2.1.4	Results for AFM Attractive Force Measurements	14
2.1.5	Results for AFM Repulsive Force Measurements on Cavities	20
3	Theoretical Calculations of Vacuum Forces	21
3.1	Summary	21
3.2	Repulsive Forces for a Rectangular Cavity with Finite Conductivity	22
3.3	Casimir Forces in Slab Geometries using Real and Inhomogeneous Materials	23
4	Gedanken Vacuum Powered Spacecraft	24
5	Newly Fabricated Materials with Negative Index of Refraction	25
6	Conclusions and direction for future work	26
7	Publications	27
7.1	Journal Papers Submitted and Published	27
7.2	Conference Articles Published	27
7.3	Presentations	28
7.4	Articles in Popular Press/Video	29
7.5	Important Recent Citations in MEMS Research to our work:	30
8	Appendix	31

Final Report: Study of Vacuum Energy Physics for Breakthrough Propulsion

G. Jordan Maclay
Quantum Fields LLC
Richland Center, Wisconsin 53581

Jay Hammer and Rod Clark
MEMS Optical, Inc.
Huntsville, Alabama 35806

Michael George, Yeong Kim, and Asit Kir
University of Alabama
Huntsville, Alabama 35805

Abstract

This report summarizes the accomplishments during a three year research project to investigate the use of surfaces, particularly in microelectromechanical systems (MEMS), to exploit quantum vacuum forces. During this project we developed AFM instrumentation to repeatedly measure Casimir forces in the nanoNewton range at 10^{-6} torr, designed an experiment to measure attractive and repulsive quantum vacuum forces, developed a QED based theory of Casimir forces that includes non-ideal material properties for rectangular cavities and for multilayer slabs, developed theoretical models for a variety of microdevices utilizing vacuum forces, applied vacuum physics to a gedanken spacecraft, and investigated a new material with a negative index of refraction.

1. SUMMARY

During this contract we focused our efforts in several areas related to vacuum forces and surfaces, with the following accomplishments:

1. development of methods and instrumentation to measure vacuum forces in the 10s of nanoNewtons with good repeatability and signal to noise ratio using an AFM (Atomic Force Microscope), operating in an excellent vacuum (10^{-6} torr).
2. obtaining cavity structures formed using X-ray photolithography and interferometry that have dimensions in the 10s and 100s of nanometers,
3. calculating repulsive forces in rectangular cavities of all aspect ratios for both perfect conductors and imperfect conductors for the first time, and determining the optimum geometries for the measurement of repulsive vacuum forces.
4. calculating vacuum forces arising from parallel slabs made from layers of materials with different dielectric functions for the first time,
5. calculating temperature dependent Casimir forces arising from the temperature dependence of the permittivity for the first time,
6. applying vacuum forces to a "gedanken spacecraft," and
7. exploring a new material with a negative index of refraction.

The experiment to measure repulsive Casimir forces is part of our three-year effort to begin to build, step by step, the knowledge base necessary for the development of engineered devices of use to the NASA mission based on quantum vacuum effects. Our objective was to develop theoretical models of elementary systems that utilize vacuum forces and energy, to understand how these models behave, and then to explore some of these models experimentally. Some of the theoretical models are discussed in [J. Maclay, "A Design Manual for Micromachines using Casimir Forces: Preliminary Considerations," Proceedings of STAIF-00 (Space Technology and Applications International Forum-2000, Albuquerque, NM, January, 2000),, edited by M.S. El-Genk, AIP Conference Proceedings 504, American Institute of Physics, New York 2000. Published in hardcopy and CD-ROM by AIP], and [J. Maclay, J. Hammer, "Vacuum forces in Microcavities," Proceedings of the Seventh International Conference on Squeezed States and Uncertainty Relations (ICSSUR), Boston, MA, June 4-6, 2001. Proceedings are now available on line at <http://www.physics.umd.edu/robot>, click on Proceedings]. Since the critical dimensions for these devices are typically micron to submicron, the experimental research utilizes microfabrication technology and the methods developed for MicroElectromechanicalSystems (MEMS).

The great difficulty of experiments involving Casimir forces was highlighted in discussions with the three most active experimental groups in the world measuring Casimir forces. These discussions took place at a conference November 14-18, 2002 in Cambridge, MA at the Harvard-Smithsonian Center for Astrophysics, where Jordan Maclay and Carlos Villarreal each presented a paper. The Italian group worked for seven (7!!) years before obtaining publishable Casimir forces for flat parallel plates. They worked for two years just to eliminate dust! The Riverside group of Mohideen says they use hundreds of cantilevers and flat surfaces until they get a good one. Mohideen's group has achieved high precision in their experiments, and developed very creative solutions to difficult experimental problems. The group at Lucent headed by Frederico Capasso (Bell Labs) says a minimum of two years is required for an experiment. The beautiful work at Lucent is particularly interesting and relevant to our efforts since they have utilized MEMS structures in their experiments.

We have come a long way in our efforts at UAH, and have developed an instrument that has an excellent signal to noise ratio, can measure surface forces with excellent repeatability in the 10s of piconewtons at a vacuum of 10^{-6} torr, which is the highest vacuum of any of the systems currently making Casimir force measurements. This instrument can serve as a platform for the measurement of Casimir forces in a variety of geometries and experiments. At this time, we are disappointed to report that the most recent data, although encouraging, is still not as good as is required. Some of the difficulties that have plagued the experiment and our efforts at their solution are the following:

1. Dust and contamination of the experimental surfaces; dust adhering to spheres on cantilever. We have tried to eliminate this problem by building a clean room around the instrument and doing all assembly in clean room environment.
2. Oxides on the surfaces of the sample fixturing trapping electrostatic charges. We hope we have eliminated oxides by coating all surfaces with a thick coating of gold. More effort may be required if large residual potentials persist.
3. Interference of laser diode light in the photodiode detector. We completely redesigned the optical system several times, but still it appears we may not have eliminated this very challenging and very persistent problem.
4. Difficulty of getting accurate gold cavities with very small dimensions. We obtained the best cavities we could from those expert in their fabrication, however the manufacture of such cavities is an art, and a major research project in itself.
5. Problems with contact resistance in applying voltages to the substrate and grounding the AFM cantilever. We tried to use very good connections to the substrate (the best seemed to be silver epoxy rather than pressure fittings) and to insure good electrical contact to the sphere by coating the sphere with gold first and then using silver epoxy to attach it to the gold coated cantilever.
6. Difficulties in getting smooth surfaces on the sphere and the substrates. We tried using the smoothest surfaces for sputtering deposition for flat substrates. We need to develop some method to get smoother spheres.

During the last three years we have made major accomplishments in the theoretical understanding and calculation of vacuum forces. Three years ago, we did numerical computations to evaluate the vacuum forces in all geometric configurations of a rectangular cavity [J. Maclay, "An analysis of vacuum fluctuation energy and Casimir forces in conductive rectangular cavities," *Phys. Rev. A.*, 61, 052110 (2000)]. We assumed, as is done in most calculations of Casimir forces for metals, an infinite conductivity at all frequencies. Only for the case of two infinite parallel plates have calculations been done using the actual material properties. Today, three years later, one of the key issues in the development of practical devices based on quantum vacuum effects, such as Casimir forces, is the effect of the real material properties, such as the dielectric function. In the last year we developed a powerful theory that gives the Casimir force for planar structures with arbitrary dielectric function, or composed of layers of different media. This theory can serve as the basis for design tool, allowing one to design a material with the desired Casimir force, within limits. IN addition we developed a theory to compute the vacuum force in a rectangular cavity as a function of the plasma frequency of the metal. The finite conductivity reduces the repulsive Casimir force, but does not dramatically alter the physics.

Our proposal to measure repulsive forces has stimulated continued discussion among researchers, and some theoretical disagreement as to how one includes the binding energy of the material, and whether it is possible to have repulsive forces between two separate surfaces. Some theorists maintain that if one imagines splitting a closed cavity, then the attractive forces where the surfaces are in close proximity will generate an attractive force that will overpower any repulsive forces. In part this argument is based on one of the usual interpretations of Casimir forces, that is that they can be viewed as originating as fluctuations within matter, as in the Lifshitz model, not in the the quantum vacuum as in the original Casimir calculation. If Casimir forces do in fact arise from fluctuations within the vacuum, then is may be that repulsive forces are observed. At this point the theory is not precise on these predictions, but interesting developments are to be expected.

At the Harvard-Smithsonian conference, Capasso said he is considering doing an experiment to measure repulsive forces, and he and his associate asked me many questions. Our theoretical presentations linking Casimir forces and MEMS in the past years have, in part, stimulated important work at Lucent Technology by Capasso's group, where MEMS devices were made and tested that verified the model of an anharmonic Casimir oscillator the PI had done in 1995. The Lucent group then used the Casimir force for the oscillating system to make a very sensitive position sensor.

Two of the stated goals of the BPP program are to sponsor credible research, subject to peer review, and to disseminate the results of the research to the broader scientific community. With BPP support, during this contract, collectively we published six journal articles, with three addition articles under review, published seven conference proceedings (three on line), and made 13 technical presentations. In addition, our work was featured in an hour long TV segment done by NHK (Japanese Public Television) on Science in the New Millennium, and featured in an article in the popular press ["Energy Unlimited," by Henry Bortman appeared in *New Scientist Magazine*, pp32-34, 1/22/2000]. Our work was mentioned in *Science News* ["Force from empty space drives a machine", *Science News*, Feb. 10, 2001, Vol. 159, No. 6, p. 86].

At the workshop we just participated in, Casimir Forces: Recent Results in Experiment and Theory, most of the key researchers in Casimir forces were present, and it was therefore a most excellent workshop. We were pleased that numerous researchers were aware of and interested in the work we have been doing.

2. DEVELOPMENT OF AFM INSTRUMENTATION

The instrument for measuring Casimir forces is based on an Atomic Force Microscope and has been developed at the University of Alabama by Prof. Michael George, Dr. Young Kim, and Dr. Asit Kir. We proposed to measure repulsive vacuum forces, which have never been measured. This experiment may have implications about the nature and origin of quantum forces as well as provide the basis for the development of new MEMS devices using Casimir forces. The experiment is done using an AFM (atomic force microscope) operating in a vacuum chamber, which is required for a precision measurement. We measure the force between a gold coated substrate and a cantilever on which we have mounted a 210 μm diameter sphere metallized with gold. When the sphere gets to within several hundred nm of the substrate, it experiences a vacuum force (called a Casimir force), which is what we are interested in observing very carefully (schematic of experiment is shown in Figure 2.1). This force is due to the change in the quantum vacuum caused by the surfaces. In order to calibrate the actual cantilever deflection and determine absolute magnitudes of the forces, we also apply a potential difference between the substrate and cantilever and measure the electrostatic deflection of the cantilever. Since we have calculated the electrostatic force exactly for this geometry using a finite element model, we can obtain an electrostatic calibration of the cantilever. Details of this experiment are given in [Maclay, J. Hammer, M. George, R. Ilic, Q. Leonard, R. Clark, "Measurement of repulsive quantum vacuum forces," AIAA-2001-3359, AIAA/ASME/SAE/ASEE 37th Joint Propulsion Conference, Salt Lake City, 2001]

The AFM instrument built at UAH for measuring Casimir forces is shown in Fig.2.2. A view of the instrument and the associated electronics is shown in Fig. 2.3. The entire system is enclosed in a clean room structure containing two laminar flow HEPA workstations as shown in Fig. 2.4. A 50 μm sphere mounted on a triangular cantilever is shown in Fig. 2.5. For all experiments we used polystyrene spheres about 200 μm in diameter on triangular cantilevers approximately 300 μm long. Fig. 2.6 shows the CCD image of a cantilever above a University of Wisconsin cavity array.

There are two parts to this experiment. The first part is to make measurements of the force between the sphere and a very flat, gold surface that are in agreement with theory. This force, which is attractive, was measured for the first time since Casimir made his original prediction half a century ago in two classic experiments in the last three years. The most accurate measurement, done by Mohideen using an AFM approach similar to ours, verified the correctness of the theory to within about 1%. During this last year we made experimental progress, eliminating most of the drift in the data and most of the slope at large separations, but we still do not have publication quality data. After Prof. George has obtained credible results for the attractive Casimir force using the flat, gold plates, he will make measurements on the cavity arrays we have obtained and characterized by SEM. One

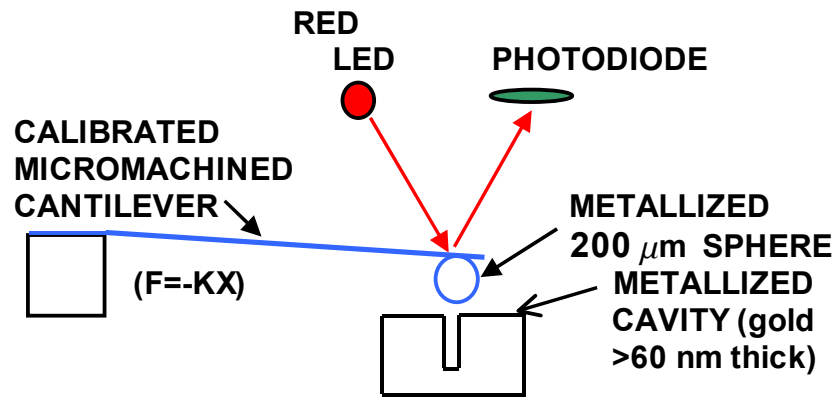


Figure 2.1: Schematic of the measurement of Casimir forces between a gold metallized sphere and a gold cavity using an Atomic Force Microscope (AFM).

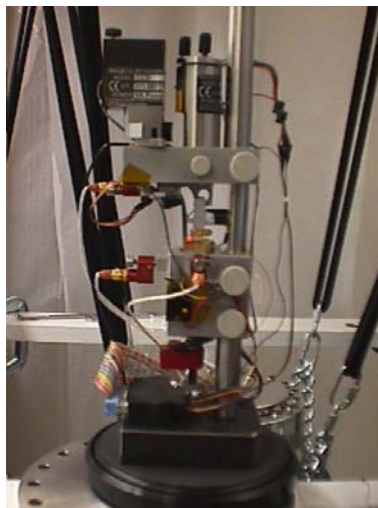


Figure 2.2: Shows one of the configurations for the AFM Casimir force microscope (CFM). Several configurations were tested during the contract. The cylinder in the upper right is the z-scanner, to its left is the CCD video camera, and below is the scanner is the stage with the sample. The red laser can be seen coming from back of the image, toward the sample rather than perpendicular through the scanner as before. On the left side of the picture and on the bottom center one can see the white cabling leading to the three piezo motors that enable x-y actuation of the sample and also of the detector while the system is in vacuum. The vacuum flange is visible at bottom of the AFM.

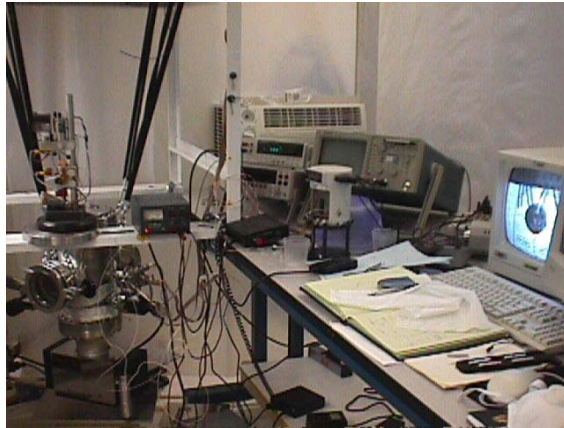


Figure 2.3: The vacuum chamber for the AFM is on the far left. The black shock cords supporting the chamber from the top of the white metal frame are visible. To the right are the electronics, including the monitor showing an image of a cantilever sphere from the CCD camera inside the vacuum chamber.



Figure 2.4: Clean room structure surrounding the AFM force measuring instrument. The structure contains two laminar flow HEPA hoods which maintain a positive pressure. The plastic walls stop about 1 inch above the ground to allow flow lines to remove dust from the cleanroom.

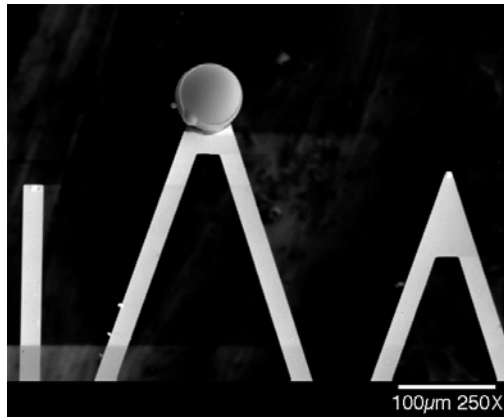


Figure 2.5: CCD image of a metallized gold sphere on the AFM cantilever in vacuum above a cavity array defined using X-ray photolithography.

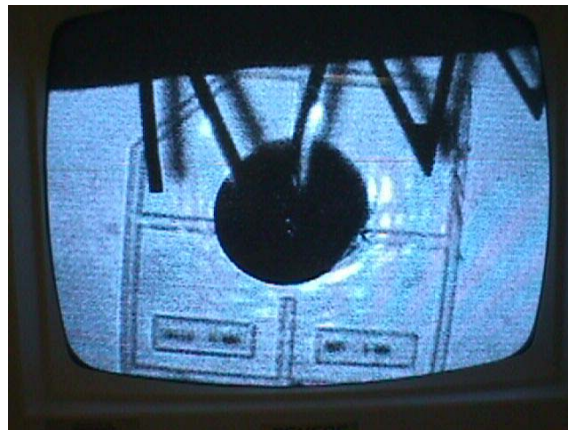


Figure 2.6: Image from a CCD camera mounted in the AFM that shows the cantilever and sphere above a test array of cavities.

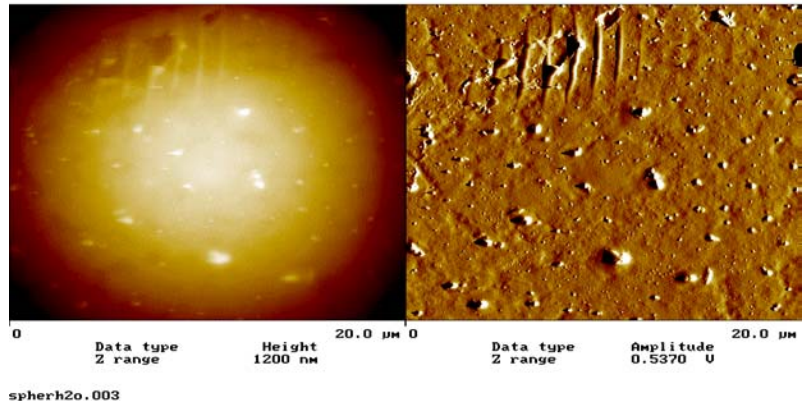


Figure 2.7: AFM image of a polystyrene sphere, showing striations, possibly due to tweezers or interference effects.

set of arrays was made using x-ray lithography at the University of Wisconsin Center for NanoTechnology and have characteristic dimensions in the hundreds of nanometers. This last year we obtained a second set of arrays from a researcher at MIT. The MIT cavity width is 40 nm, which is very narrow, and a wall thickness of 60 nm. Based on the theoretical calculations we have done, it is possible that we may observe a repulsive force for these very narrow cavities.

2.1. Experimental Methods

We briefly mention some of the experimental issues of some importance to one entering this field.

2.1.1. Assembly of Cantilevers

Fig. 2.7 shows what may be additional roughness on a polystyrene sphere, possibly induced by the use of tweezers or other fixtures to hold the sphere.

The rms roughness of a gold metallized sphere is shown to be about 12.8 nm in the AFM image Fig. 2.8. Cleanliness of the process is also an issue, as can be seen in the SEM image Fig. 2.9 in which inhomogenities can be seen as the white specs on the surface of the sphere mounted on an AFM cantilever with silver epoxy. Another surprising problem occurred during Casimir force measurements of which we remained unaware until Dr. Kim did an AFM of the sphere after the measurements were complete, as shown in Fig. 2.10. It is important to fully characterize the spheres after mounting, and sometimes after the measurements are complete.

2.1.2. Cavity Substrates

Making cavity structures is very difficult since the features are small, in the 50-100 nm range, and the aspect ratios are comparatively large, about 4 or more. We obtained cavities from

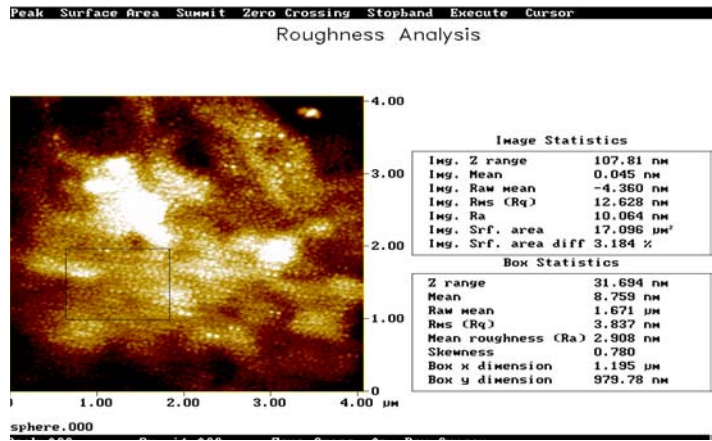


Figure 2.8: AFM image and analysis of the surface of a polystyrene sphere. The rms roughness is about 12 nm.

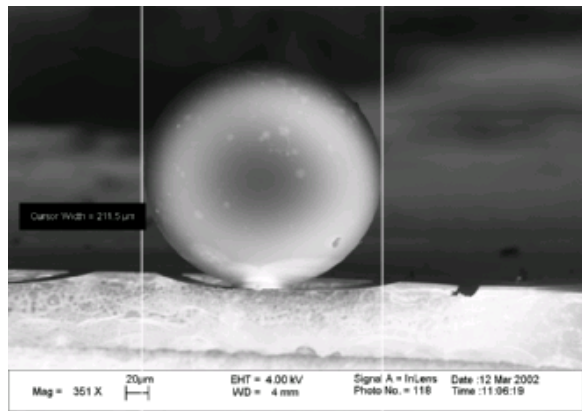


Figure 2.9: SEM image of a gold coated polystyrene sphere mounted on an AFM cantilever.

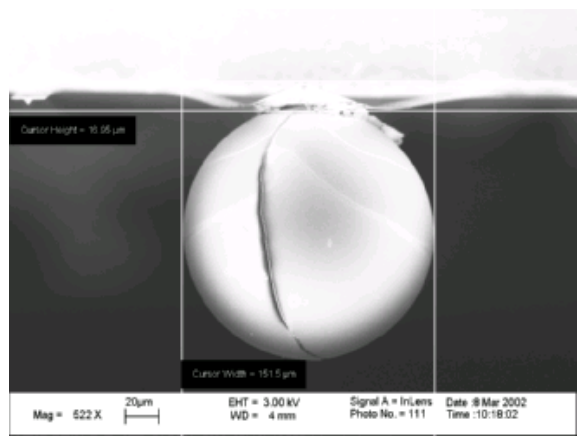


Figure 2.10: SEM image of a gold coated polystyrene sphere with a fracture mounted on an AFM cantilever.

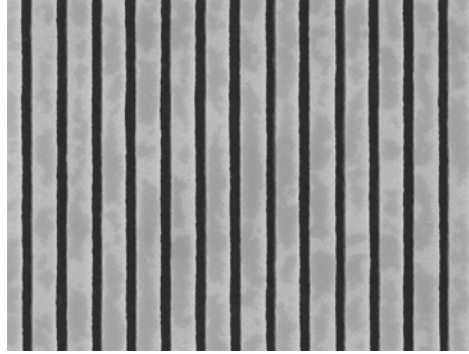


Figure 2.11: SEM of the gold array made at the University of Wisconsin Center of Nanotechnology. The dark regions are cavities about 125 nm across and 500 nm deep. The white regions are the walls about 225 nm thick. Each cavity is 100 μm long.

Prof. France Cerrina, Director of the University of Wisconsin Center for Nanotechnology, that were fabricated using X-ray photolithography. The structures are essentially long narrow gratings. The wall or lines are about 225 nm thick, and the cavities or lines are about 125 nm across. The depth is 500 nm. The geometry is well formed, as shown in Fig. 2.11. Although a precise measurement of the surface forces with such a grating would provide new and very interesting information, our theoretical model predicts that the features sizes need to be reduced to measure a net repulsive forces as opposed to a reduced attractive force.

We were able to obtain cavity substrates from Prof. H. Smith at MIT, who uses an interferometric method to fabricate narrow line gratings. We obtained a 10 X. 20 mm. substrate with a gold grating structures, with a cavity width of 40 nm, a wall thickness of 60 nm, and a depth of about 160 nm. This is a very narrow cavity formed using optical interference methods. Several AFM images of the cavities are shown below. Fig. 2.12 shows a view over a 500 nm square region. The image on the left is the usual AFM height mode image that gives a good indication of the surface topography. On the right is the equivalent of the DI (Digital Image Inc.) tapping mode image, which gives a good indication of the immediate region of the surface but with little sensitivity to the large scale variations in overall surface height. The image from this mode is obtained from the shift in the resonant frequency of the vibrating cantilever as it nears the surface.

The data in the last image may be presented quantitatively as a scan across the cavity, as shown in Fig. 2.13. This scan shows that in addition to the surface roughness corresponding to the presence of the cavities, there is a roughness of several nm.

A SEM of the cavity Fig. 2.14 shows that the walls may not be of uniform thickness, and may be thicker at the top. From the SEM scale, the openings are close to the nominal 40 nm. Based on the AFM images and SEM images, it appears that the cavity openings may not be as well defined as we would prefer, although it is difficult to interpret the SEM and AFM data very accurately. It is difficult to make such small structures with such high aspect ratios.

In order to measure the parallel plate Casimir force we have made flat gold surfaces using

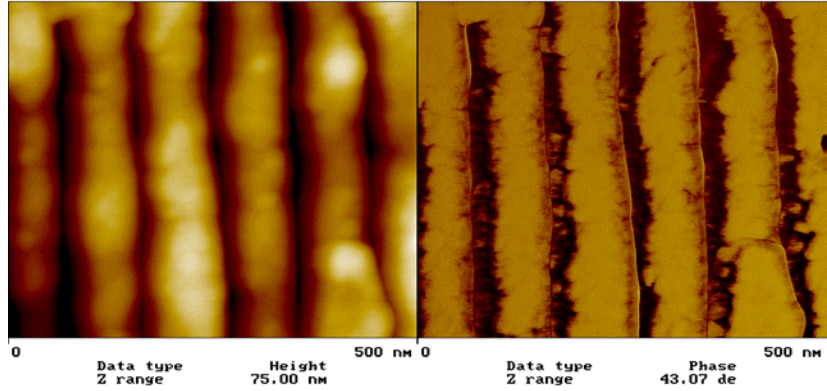


Figure 2.12: AFM image of a gold grating structure, formed with a spacing or cavity width of 40 nm, a line or wall thickness of 60 nm, and a depth of about 160 nm.

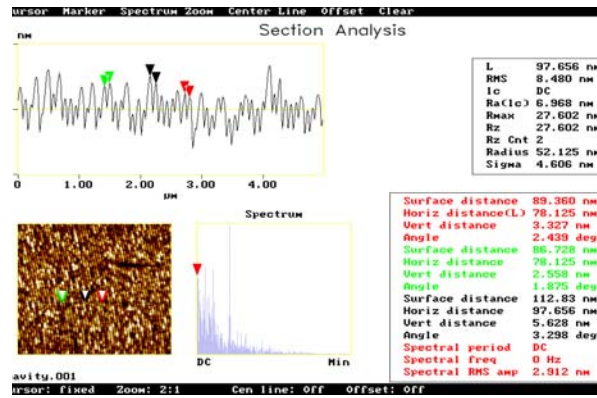


Figure 2.13: Surface roughness analysis for the cavity from MIT shown in Fig. 2.12.

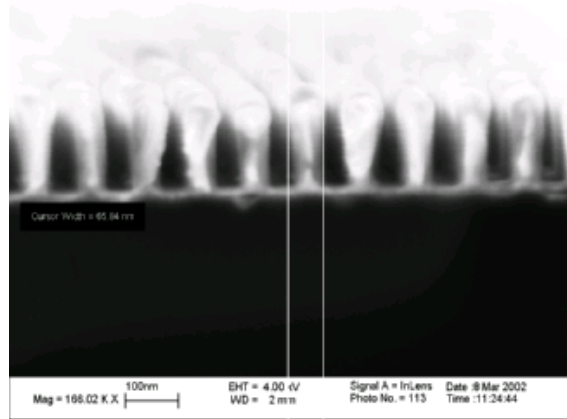


Figure 2.14: SEM image of cavity array from MIT. The walls are nominally 60 nm thick, the cavities are nominally 40 nm wide.

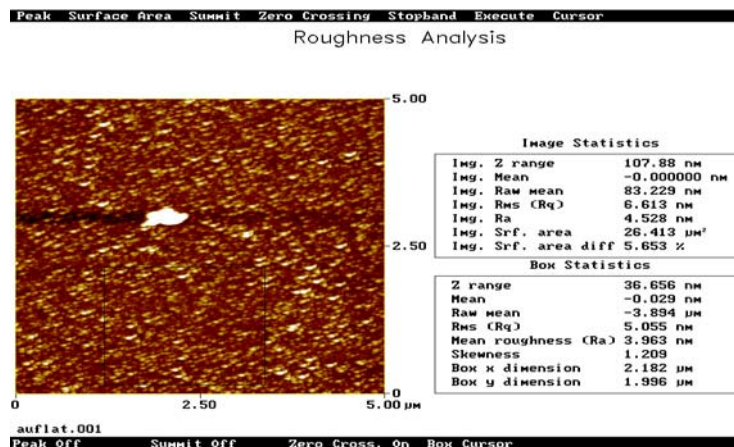


Figure 2.15: AFM roughness analysis for a flat gold surface used in the measurement of the Casimir force between flat surfaces.

silicon wafers or sapphire optical flats, or cleaved mica. The roughness is typically about 5 nm as shown in Fig. 2.15.

2.1.3. Electrostatic Calibration

The electrical wiring and grounding was checked, and a new voltage source installed. The voltage is applied to the substrate, measured with a separate voltmeter, while the AFM cantilever is at ground potential. Calculations were done by Jay Hammer of MEMS Optical of the theoretical electrostatic force using a finite element model. In the model he considered an array of 18 cavities, which gave a result that was insensitive to adding more cavities.

2.1.4. Results for AFM Attractive Force Measurements

As an indicator of the proper functioning of the UAH AFM instrument, we first are endeavoring to reproduce the know results for the Casimir force between a gold sphere and a flat gold plate. Curves showing the variation of the photodiode signal versus the relative separation between the plate and sphere are shown in Fig. 2.16. These curves are the result of averaging 30 runs and show a excellent signal/noise ratio. However, note that there is a periodic component to the signal present in all curves. The noise level is much less than the amplitude of the interference component. This periodic signal is very visible if we plot the signal for low photodiode signals. This periodic component may be due to interference effects in the LED beam. It is greatly reduced from what it was last year, but is still a problem at the level of precision this measurement is approaching as can be seen in Fig. 2.17.

The photodiode signal is due to the combined Casimir and electrostatic force. By equating the difference, for example, between the curve for 61 mV and the curve for 0 mV, to a theoretical electrostatic force, we can obtain a set of equations that best fit the data and provide the calibration information. The fit of a theoretical electrostatic force to the difference curve for the data at 61 mV and 0 mV applied voltage is shown in Fig. 2.18.

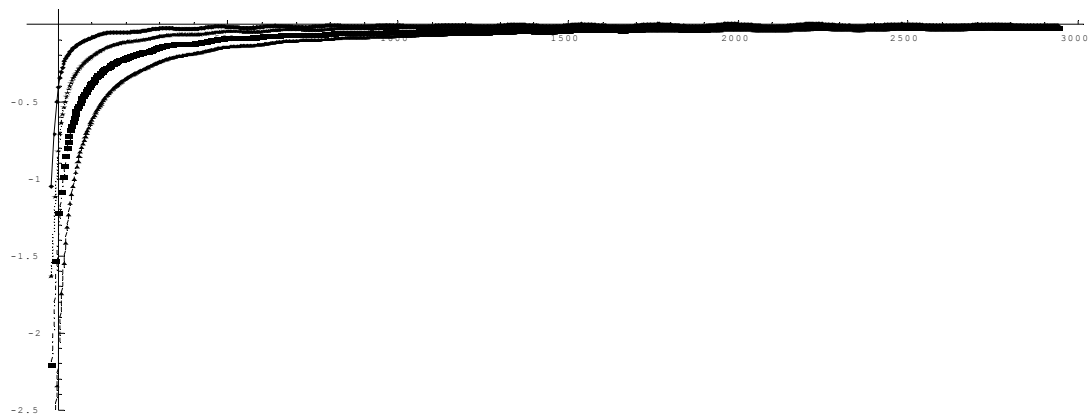


Figure 2.16: AFM curves of the photodiode signal versus the nominal relative separation between the gold sphere and the flat gold plate. The top curve is for zero applied bias, the next three from top to bottom with applied biases of 61 mv, 121 mv, 161 mv, respectively.

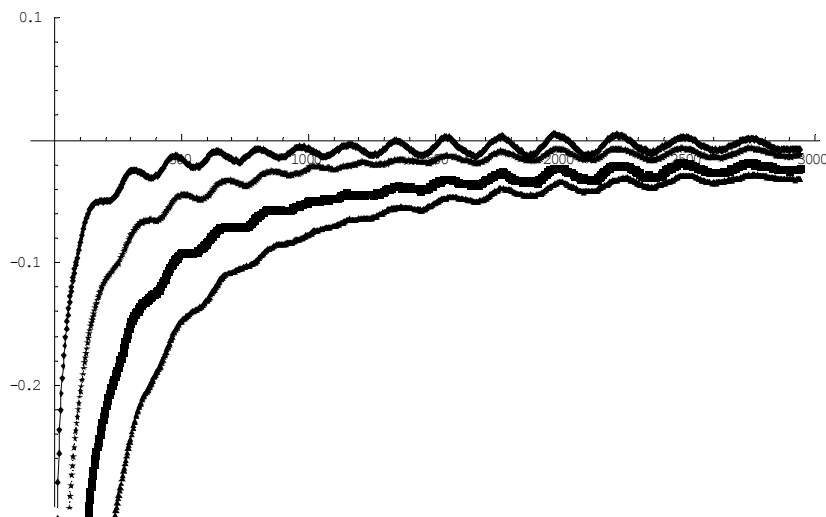


Figure 2.17: AFM photodiode signal versus separation for the data shown in the previous figure, plotted for low values of the photodiode signal.

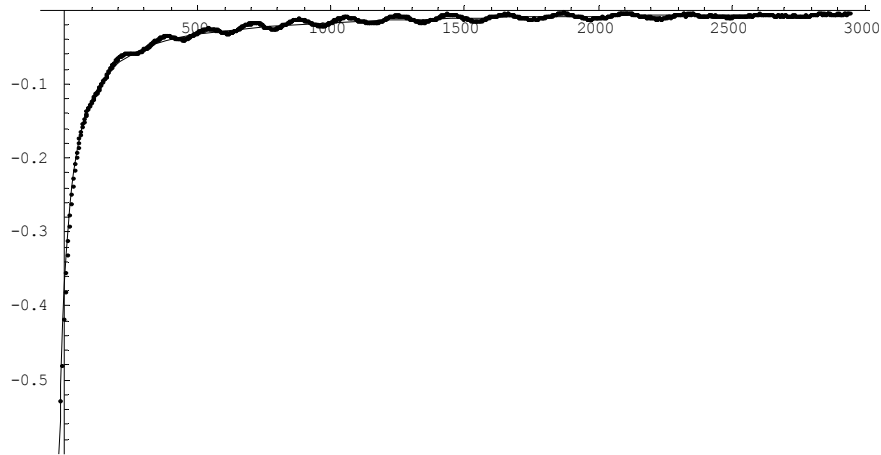


Figure 2.18: Theoretical fit (solid line) to the electrostatic force between a gold sphere and a flat gold surface. This is the electrostatic force obtained as the difference between the measured curves at 60 mV and 0 mV, respectively.

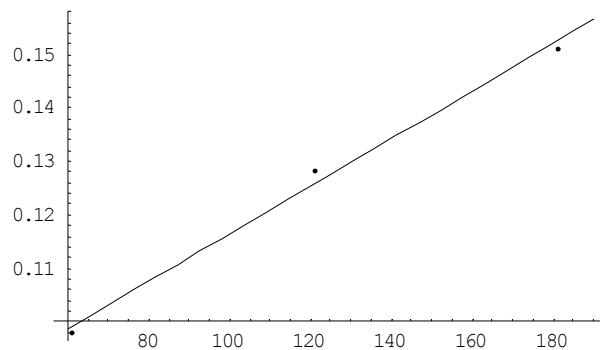


Figure 2.19: Electrostatic fit coefficient/voltage vs applied voltage for the three voltages.

By doing a similar fit for the data at all applied voltages, we find the best values of the residual potential, the cantilever calibration, and the absolute separation. The three fits indicate that we need to shift the relative separation by a distance of 49.6 nm, 53.9 nm, 52.9 nm, respectively to obtain the absolute separation. The average shift is 52.1 nm, which corresponds to a distance of closest approach of 33 nm. It is very encouraging that the scatter in the shifts is very small, about 4 nm. In order to obtain the built in potential and the force constant, we do a least squares fit to a plot of the overall fit coefficients divided by the applied voltage vs the applied voltage as shown in Fig. 2.19. The x - intercept/2 is the built in potential -80.6 mV. The slope corresponds to a force constant of $mconf1016 * kpdf1016 = 0.0400 \mu\text{N}/\mu\text{m}$. With these parameters we can determine the absolute force corresponding to a photodiode signal, correct for the residual potential, and obtain the final expression for the Casimir force.

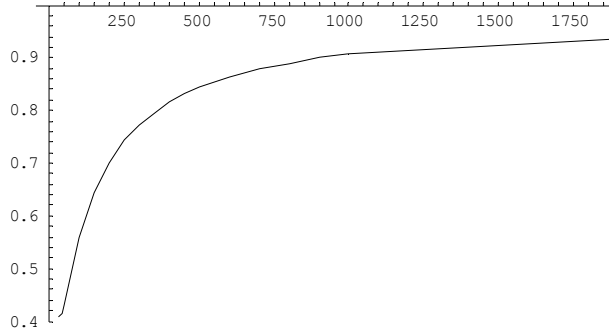


Figure 2.20: Multiplicative force correction for gold in parallel plate-sphere geometry.

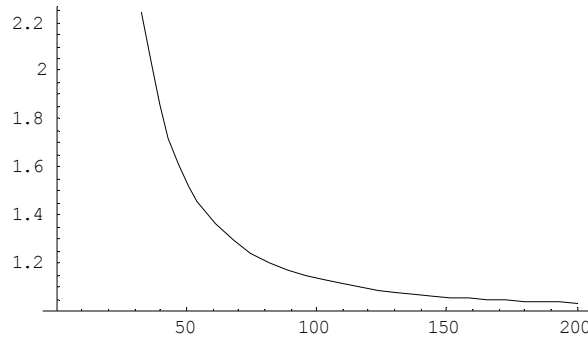


Figure 2.21: Multiplicative correction to the Casimir force for a RMS roughness of 15 nm.

We need to be able to compare the data to a theoretical expression for the Casimir force for a gold surface. A multiplicative correction for finite conductivity was computed by Astrid et al and is plotted in Fig. 2.20. Corrections must also be made for the surface roughness. The roughness correction really depends on the detailed distribution of the various height regions on the surface. If we assume a normal distribution, we can approximate the multiplicative correction as a polynomial. The correction is plotted for a roughness of 15 nm as a function of the (maximum) separation in nm in Fig. 2.21. For a roughness this large, the correction is quite large. Ideally the roughness should be below 5nm, and the correction is then just several percent. We need to process the spheres so that the roughness is reduced. Using the conductivity correction for gold, the roughness correction, and the expression for the ideal Casimir force for a sphere and a flat plate, we can make a theoretical prediction to plot with the measured Casimir force. The theoretical result (solid line) and experimental result (points) for a measurement of the Casimir force between a gold metallized sphere 220 μm in diameter and a flat gold surface are shown in Fig.2.22. Plotting just the region for separation less than 500 nm shows the disagreement between theory and experiment more clearly in Fig. 2.23. The agreement is not too bad when we consider that there are no arbitrary fitting parameters, and that the curve for the Casimir force follows precisely from the data shown in the previous figure. In the computations, we have made a correction for the surface roughness. By AMF measurement, the rms roughness for the sphere is 6 nm and 12 nm for the gold plate. The corresponding corrections are significant, about a factor of 2 at the distance of closest separation. The experimental and theoretical curves agree more

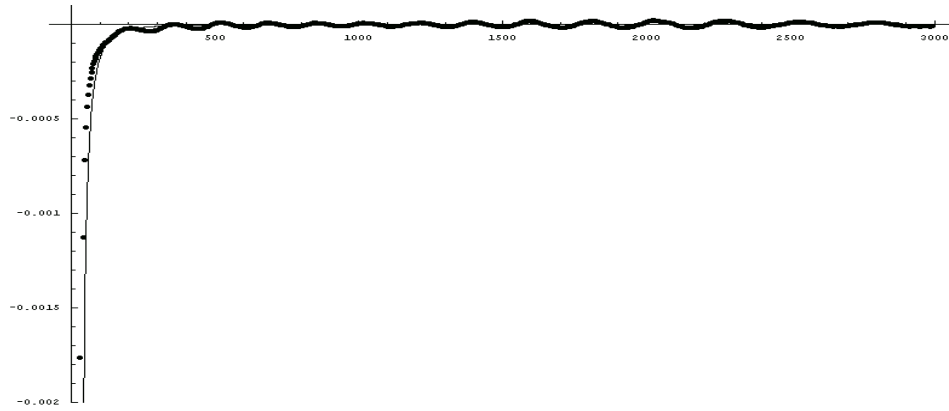


Figure 2.22: Plot of the force in nN versus the separation in nN for a gold metallized sphere near a flat gold surface. The data curve is to the left, the theoretical calculation to the right. The surface roughness is assumed to be 12 nM, and corrections for the conductivity of gold have been included.

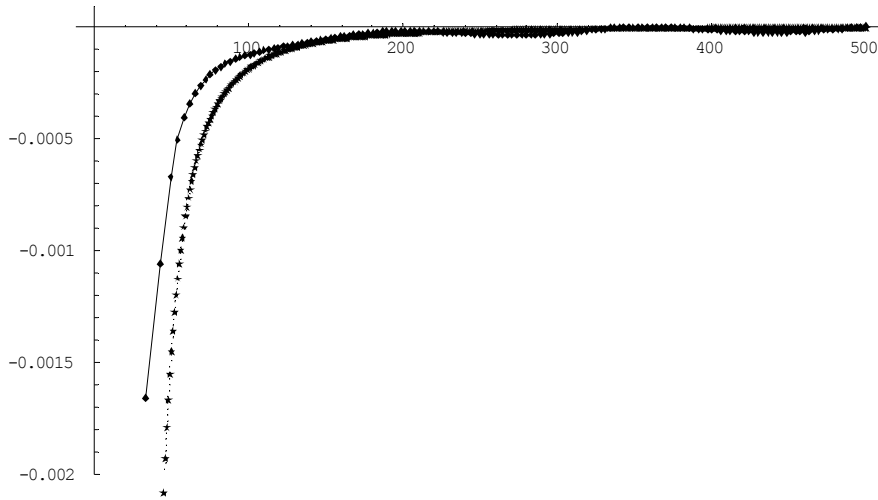


Figure 2.23: Plot of the force in nN versus the separation in nN for a gold metallized sphere near a flat gold surface. The data curve is to the left, the theoretical calculation to the right. The surface roughness is assumed to be 12 nM, and corrections for the conductivity of gold have been included.

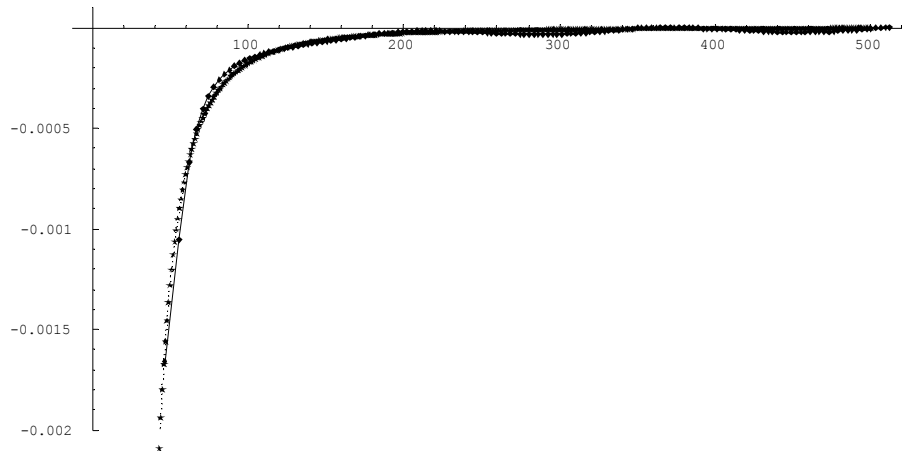


Figure 2.24: The data in the previous figure has been shifted 13 nm to the right to make the calculation and measured values agree more closely.

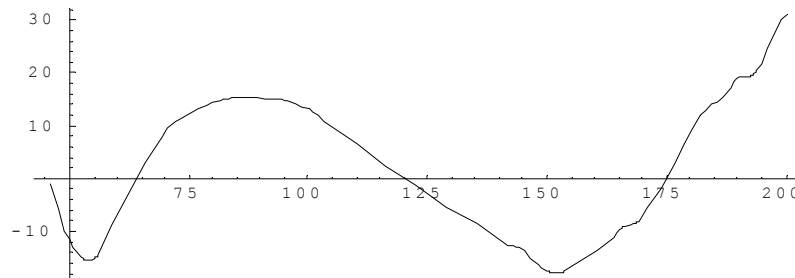


Figure 2.25: The percent deviation between the measured and calculated values for the data plotted in the previous figure, shown as a function of the separation.

closely if we arbitrarily assume that the data points should be shifted about 13 nm to the right, as shown in Fig. 2.24. After this shift, the fit is much better, however, a residual error remains that varies approximately periodically between about +15% and -15%. as shown in Figure 2.25. This error is much larger than the precision in the data, and is probably due in part to a systematic error, for example the periodic interference in the photodiode signal.

Comments on Current Results

These experiments are very difficult. The other groups engaged in such measurements have spent a minimum of two years (Bell Labs and Riverside groups), and a maximum of 7 years (Italian group).before obtaining data for a given experiment. The data we have obtained after about two years is therefore very encouraging. The current thrust of the work at UAH is to improve the smoothness of the samples, getting it in the nm range instead of the 10 nm range where it currently is, and to improve the cleanliness of the samples.

The periodic noise appears to be due to an interference of the laser diode beam reflected

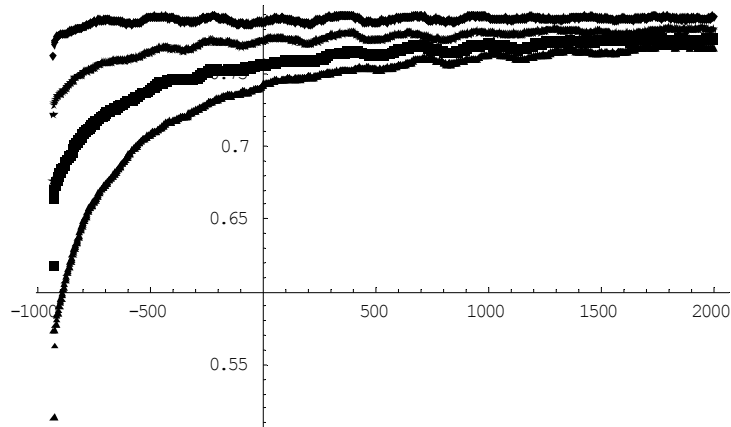


Figure 2.26:

off the cantilever with another component of the beam reflected off a stationary source, probably the lens in the optical system. Such an interference would be expected to give maxima that are separated by a distance of $1/2$ the wavelength of the laser diode or about 325 nm. However, the maxima are separated by about 150 nm, or half the expected distance. Perhaps this arises from multiple reflections. Much effort has gone into trying to eliminate this interference. As soon as this is accomplished, we will be able to make credible measurements of the cavity arrays to determine the nature of corresponding vacuum forces.

2.1.5. Results for AFM Repulsive Force Measurements on Cavities

Measurements were made of the force between the gold metallized sphere on the AFM and cavities made by University of Wisconsin and the cavities made at MIT. In both cases, we did not observe a net repulsive force. The raw data for the most recent measurements 11/08/02 on the MIT cavities are shown in Fig. 2.26 for applied voltages ranging from 0 to 160 mv. The periodic interference appears to have a significant effect on the shape of the highest curve, 0 mv, which will cause errors in the derived Casimir force. Until we can obtain good results with the parallel plate experiment, we are not confident of our results with other geometries.

3. THEORETICAL CALCULATIONS OF VACUUM FORCES

3.1. Summary

In the first year of this effort, we computed and analyzed the vacuum forces in a perfectly conducting rectangular cavity, giving us a good knowledge base to move forward [J. Maclay, "An analysis of vacuum fluctuation energy and Casimir forces in conductive rectangular cavities," *Phys. Rev. A.*, 61, 052110 (2000)]. We determined the optimum geometries for the measurement of repulsive forces, and developed a corresponding experiment and an approximate theory [Maclay, J. Hammer, M. George, R. Ilic, Q. Leonard, R. Clark, "Measurement of repulsive quantum vacuum forces," AIAA-2001-3359, AIAA/ASME/SAE/ASEE 37th Joint Propulsion Conference, Salt Lake City, 2001]. We then used our knowledge about the theoretical forces in rectangular cavities to explore some gedanken machines [J. Maclay, "A Design Manual for Micromachines using Casimir Forces: Preliminary Considerations," Proceedings of STAIF-00 (Space Technology and Applications International Forum-2000, Albuquerque, NM, January, 2000); J. Maclay, J. Hammer, "Vacuum forces in Microcavities," Proceedings of the Seventh International Conference on Squeezed States and Uncertainty Relations (ICSSUR), Boston, MA, June 4-6, 2001].

Our work stimulated other scientists to consider the question of repulsive forces in real systems, and the meaning of the theoretically calculated stress-energy tensor in QED. We explored some approximate calculations of Casimir forces, and the meaning of the repulsive forces computed for a sphere, in collaboration with Gabriel Barton, who has suggested that the discarded divergent energy terms representing intermolecular forces may overpower any repulsive forces in certain experiments [J. Maclay, P. Milloni, H. Fearn, "Of some theoretical significance: implications of Casimir effects," *European Journal of Physics* 22, 463-469, 2001].

In our proposed experiment, the cavity structure is open, and some physicists maintain that this causes the repulsive force to disappear, or attractive forces at the edge to dominate. On the other hand, no one has yet calculated the Casimir force for this geometry. In the approximate calculation we did, we included the attractive Casimir force from the edges of the cavity, as well as the repulsive force from the cavity. With improvements in theory and experiment, we may find the force may depend on the separation and the details of the experiment. As mentioned previously, the results of experiments to measure repulsive forces might have implications regarding the source of vacuum fluctuations. At this time it is too early to make any definite conclusion because exact theoretical calculations using the different models of vacuum energy for the proposed experiment have not been done.

Our work then focused on developing more realistic model for the materials, including the finite conductivity and the methods of measuring the forces [Jordan Maclay, and Car-

los Villarreal, " A Model for Casimir Forces in Closed Cavities with Finite Conductivity," presented at the symposium Casimir Forces: Recent Results in Experiment and Theory, Harvard-Cambridge Center for Astrophysics, Harvard University, Cambridge, MA, Nov. 14, 2002]. We determined that finite conductivity reduces the forces, but does not dramatically alter the physics. To allow for materials with arbitrary dielectric function, Carlos Villarreal and his collaborators developed new methods for computing forces for planar and spherical geometries [R. Esquivel-Sirvent, C. Villarreal, G. Coccoletzi, "Superlattice-mediated tuning of Casimir forces," Phys. Rev A 64, 052108 (2001), R. Esquivel-Sirvent, C. Villarreal, and W. L. Mochan., "Casimir Forces in nanostructures," Physica Status Solidi(b) 230, 409 (2002)]. Stimulated by the possibility of experiments with non-planar geometries, other theoretical groups began exploring the divergences that arise from the assumption of perfect corners, and attempting to develop more realistic representations of surfaces and corners and thereby eliminate some of the divergences that appear in the calculations. Several new approaches are being developed that avoid the idealization of infinitely sharp boundaries that implicitly require very large amounts of energy to sustain.

We now briefly discuss some of our results that have not yet appeared in the literature.

3.2. Repulsive Forces for a Rectangular Cavity with Finite Conductivity

Carlos Villarreal and the PI presented a paper describing a QED based theory to compute vacuum energy and force for rectangular metal cavities of length a , width b , height c that have finite conductivity at the symposium "Recent Developments in Experiment and Theory" held at the Harvard-Smithsonian Center for Astrophysics in Cambridge, Nov. 14-16, 2002. In our approach, we compute the energy density and the pressure on the walls of the rectangular cavity as a function of a cut-off frequency. Above the cut off frequency, we assume there is an exponentially decreasing effect of the vacuum fluctuations. Physically the cut off frequency acts like the plasma frequency of a real metal. The electrons in a metal are not able to respond faithfully to electric fields that have frequencies above the plasma frequency, consequently for frequencies above the plasma frequency, the metal is transparent. The most important result from our calculations, the prediction of a repulsive force for our geometry, seems to be a robust conclusion since it does not depend on the magnitude of the plasma frequency cut off. For the MIT cavities the predicted effect of the conductivity of gold is to lower the repulsive force by about 30% as shown in Fig. 3.1.

One of the important topics that we brought up in our presentation at the Symposium in Cambridge was the specific way in which one might measure the repulsive force. Indeed, there is no method that was acceptable to all scientists present at the conference. The approach we have proposed this last year, using an AFM sphere near an open array of cavities has the drawback that the cavities are not really closed. In this approximation, we not sure of precisely what one should measure since no one has yet made an exact calculation for such an open structure. On the other hand, one could measure the deformation of a wall in a closed cavity, the stress being due to the vacuum stress or alternatively to an experimentally applied force. Such a measurement has the advantage of involving closed cavities, but the added complication that one must consider the detailed material properties.

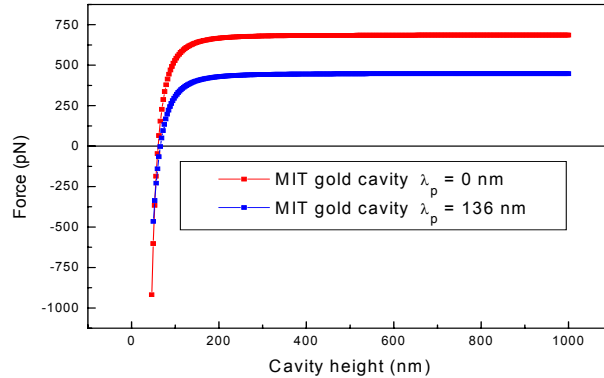


Figure 3.1: Total force on the top of a cavity 40 nm wide and 100 μm long, as a function of the depth of the cavity, for a cavity made of gold (bottom curve) and made of a perfect conductor (top curve).

Our discussions regarding repulsive Casimir forces over the last few years have focused attention and stimulated discussion in the scientific community. Recently we have highlighted the uncomfortably large gap between most theoretical Casimir force calculations and the conceptual methods by which one might measure Casimir forces in various geometries.

3.3. Casimir Forces in Slab Geometries using Real and Inhomogeneous Materials

Carlos Villarreal and his collaborators have developed powerful methods to predict the Casimir force for slabs that are formed from multiple layers of various materials, for example dielectrics and metals. The force is given in terms of a frequency dependent reflectivity of the slabs. The metals were characterized by a dielectric function in the Drude approximation, and the dielectrics by the Lorentz approximation, although other behavior is possible since they do a numerical integration. They also have considered spherical geometries using the proximity force approximation. This approach is very helpful for the design of future MEMS devices that are based on Casimir forces. With the machinery they have developed, one could, within limits, tailor a desired force distance function.

This work is described in several papers that credit the BPP program with partial support: C. Villarreal, R. Esquivel-Sirvent, and G. H. Coccoletzi, "Modification of Casimir forces due to band gaps in periodic structures," *International Journal of Modern Physics A* 17, 798 (2002), R. Esquivel-Sirvent, C. Villarreal, and W. L. Mochan., "Casimir Forces in nanostructures," *Physica Status Solidi(b)* 230, 409 (2002), and W. L. Mochán, R. Esquivel-Sirvent, and C. Villarreal, "On Casimir forces in media with arbitrary dielectric properties," *Revista Mexicana de Física* 48, 339 (2002). It was also discussed at the Harvard-Cambridge symposium: Carlos Villarreal, "Casimir Forces in Non-Homogeneous Planar and Spherical Systems," presented at the symposium *Casimir Forces: Recent Results in Experiment and Theory*, Harvard-Cambridge Center for Astrophysics, Harvard University, Cambridge, MA, Nov. 14, 2002.

4. GEDANKEN VACUUM POWERED SPACECRAFT

An attempt to address some of the key issues of the BPP program using the properties of the quantum vacuum was made in a collaboration between the PI and Robert L. Forward. A paper has been submitted for publication. A Gedanken spacecraft is described that is propelled by means of the dynamic Casimir effect, which describes the emission of real photons when a conducting surface is moved in the vacuum with a high acceleration. The maintenance of the required boundary conditions at the moving surface requires the emission of real photons, sometimes described as the excitation of the vacuum. The recoil momentum from the photon exerts a force on the surface, causing an acceleration. If one imagines the moving surface is attached to a spacecraft, then the spacecraft will experience a net acceleration. Thus we have a propellantless spacecraft. However, we do have to provide the energy to operate the vibrating mirror. In principle, it is possible to obtain this power from the quantum vacuum, and this possibility is explored. Unfortunately with the current understanding and materials, the acceleration due to the dynamic Casimir effect is very small, on the edge of measurability.

One of the objectives in this paper is to demonstrate that some of the unique properties of the quantum vacuum may be utilized in a gedanken spacecraft. We have demonstrated that it is possible, in principal, to cause a spacecraft to accelerate due to the dissipative force an accelerated mirror experiences when photons are generated from the quantum vacuum. Further we have shown that one could in principal utilize energy from the vacuum fluctuations to operate such a vibrating mirror assembly. The application of the dynamic Casimir effect and the static Casimir effect may be regarded as a proof of principal, with the hope that the proven feasibility will stimulate more practical approaches exploiting known or as yet unknown features of the quantum vacuum. A model gedanken spacecraft with a single vibrating mirror was proposed which showed a very unimpressive acceleration due to the dynamic Casimir effect of about $3 \times 10^{-20} \text{ m/s}^2$ with a very inefficient conversion of total energy expended into spacecraft kinetic energy. Employing a set of vibrating mirrors to form a parallel plate cavity increases the output by a factor of the finesse of the cavity, 10^{10} , yielding an acceleration per meter squared of plate area of about $3 \times 10^{-10} \text{ m/s}^2$ and a conversion efficiency of about 10^{-16} . After 10 years at this acceleration, a one square meter spacecraft would be traveling at 0.1 m/s. Although these results are rather unimpressive, it is important to remember this is a proof of the principal, and to not take our conclusions regarding the final velocity in our simplified models too seriously. The choice of numerical parameters is a best guess based on current knowledge and can easily affect the final result by 5 orders of magnitude. In about 1900 an article was published in Scientific American proving that it was impossible to send a rocket, using a conventional propellant, to the moon. The result was based on the seemingly innocuous assumption of a single stage rocket.

5. NEWLY FABRICATED MATERIALS WITH NEGATIVE INDEX OF REFRACTION

In the last several years materials that have a negative index of refraction in a narrow frequency band in the microwave have been developed using microfabrication methods. These materials have very unusual properties that might be of interest in the BPP mission and therefore we conducted a preliminary investigation. A classical electromagnetic wave analysis of negative index materials indicates that: 1) the momentum of a photon is in the opposite direction of the Poynting vector, which is the direction the light is propagating; 2) if light reflects off a surface, the force on the surface is toward the source of the light rather than away from it; 3) the Doppler effect is reversed, the frequency shift is negative (to lower frequencies) if the source is moving toward the detector; 4) Snell's Law applies, but the light wave bends in the opposite direction as for a normal medium. An open question is what happens to the Casimir force if a negative index material is between two plates. If the material had a negative index for wavelengths near twice the separation between the plates, then it is conceivable that the force would be attractive. One of the complications for Casimir forces is that one needs to integrate over a wide frequency region to obtain the force, and over most of this spectral range, the index will be positive.

We did the first theoretical investigation into negative index phenomena using a quantized field representation. We examined several of the predicted properties, such as the Doppler shift, and the use of negative index materials as near perfect lenses. A paper, "Quantized Field Description of Light in Negative-Index Media," by Peter Milonni and Jordan Maclay has been submitted for publication.

6. CONCLUSIONS AND DIRECTION FOR FUTURE WORK

Ten years ago many researchers in quantum physics and Casimir forces were working on rather unphysical issues, such as Casimir forces due to different topologies, or Casimir forces in various dimensional spaces, or for various fields, not the usual electromagnetic field in three dimensions. It seemed that there was not a great interest in the more mundane world of precision measurements of Casimir forces. Then several breakthrough measurements were done, by Lamoroux and Mohideen, that verified the basic theory, and gave the hope of providing a testing ground for more precise and realistic calculations.

During the course of this three year effort, there has been an increasing interest among physicists regarding the possible behavior of real systems designed to measure and exploit forces arising from the quantum vacuum. There is an increased interest in the behavior of real materials, with real boundary conditions. Two important experiments, done by the Lucent group, used MEMS structures to measure and exploit vacuum forces. The behavior of these structures was modeled in our earlier work. Several groups experienced in Casimir measurements are interested in measuring repulsive forces.

We think this trend will continue, and even accelerate as more measurements are done of Casimir forces. More devices will be built, with new modes of operation. As an indication of this trend, I was just asked to serve as a referee for a review of new phenomena at nanometer scales, including quantized heat flow, charge discreteness and the Casimir effect, and how these phenomena impact nanoscale electromechanical devices. As knowledge of Casimir phenomena increases and disseminates into engineering areas, commercially valuable devices will probably emerge. Researchers will continue their efforts at exploring the boundaries of predictions based on current theories. It may be that new experiments, perhaps involving repulsive forces, will shed new light on our understanding of vacuum forces and open new possibilities.

We strongly recommend that NASA stay abreast of these developments, and consider the implications with respect to the mission of NASA, especially the BPP program. It is very possible, that new developments may provide the basis for significant progress in reaching the BPP objectives.

7. PUBLICATIONS

7.1. Journal Papers Submitted and Published

1. Jordan Maclay and Robert L. Forward, "A Gedanken Spacecraft that accelerates by pushing on the vacuum (Dynamic Casimir Effect), submitted for publication to Physics Letters A. In Appendix 1.
2. Jordan Maclay, and Carlos Villarreal, " A Model for Casimir Forces in Closed Cavities with Finite Conductivity," submitted for publication to Physics Letters A. In Appendix 1.
3. P. Milonni, and J. Maclay, "Quantized-Field Description of Light in Negative-Index Media," Submitted to Physical Review A. In Appendix 1.
4. J. Maclay, "An analysis of vacuum fluctuation energy and Casimir forces in conductive rectangular cavities," Phys. Rev. A., 61, 052110 (2000).
5. R. Esquivel-Sirvent, C. Villarreal, G. Coccoletzi, "Superlattice-mediated tuning of Casimir forces," Phys. Rev A 64, 052108 (2001)
6. J. Maclay, P. Milloni, H. Fearn, "Of some theoretical significance: implications of Casimir effects," European Journal of Physics 22, 463-469, 2001
7. R. Esquivel-Sirvent, C. Villarreal, and W. L. Mochan., "Casimir Forces in nanostructures," Physica Status Solidi(b) 230, 409 (2002).
8. C. Villarreal, R. Esquivel-Sirvent, and G. H. Coccoletzi, "Modification of Casimir forces due to band gaps in periodic structures," International Journal of Modern Physics A 17, 798 (2002).
9. W. L. Mochán, R. Esquivel-Sirvent, and C. Villarreal, "On Casimir forces in media with arbitrary dielectric properties," Revista Mexicana de Física 48, 339 (2002).

7.2. Conference Articles Published

1. J. Maclay, "Unusual Properties of Conductive Rectangular Cavities in the Zero Point Electromagnetic Field: Resolving Forward's Casimir Energy Extraction Cycle Paradox," "Space Technology and Applications International Forum 1999," Albuquerque, NM, Feb., 1999, El-Genk, M. S., ed, American Institute of Physics Conference Proceedings 458.

2. J. Maclay, "A Design Manual for Micromachines using Casimir Forces: Preliminary Considerations," Proceedings of STAIF-00 (Space Technology and Applications International Forum-2000, Albuquerque, NM, January, 2000), edited by M.S. El-Genk, AIP Conference Proceedings 504, American Institute of Physics, New York 2000. Published in hardcopy and CD-ROM by AIP.
3. Maclay, J. Hammer, M. George, R. Ilic, Q. Leonard, R. Clark, "Measurement of repulsive quantum vacuum forces," AIAA-2001-3359, AIAA/ASME/SAE/ASEE 37th Joint Propulsion Conference, Salt Lake City, 2001
4. J. Maclay, J. Hammer, "Vacuum forces in Microcavities," Proceedings of the Seventh International Conference on Squeezed States and Uncertainty Relations (IC-SSUR), Boston, MA, June 4-6, 2001. Proceedings are now available on line at <http://www.physics.umd.edu/robot>, click on Proceedings. In Appendix.
5. Jordan Maclay, and Carlos Villarreal, "A Model for Casimir Forces in Closed Cavities with Finite Conductivity," presented at the symposium Casimir Forces: Recent Results in Experiment and Theory, Harvard-Cambridge Center for Astrophysics, Harvard University, Cambridge, MA, Nov. 14, 2002. This presentation will be available shortly on line at ITAMP (Institute of Theoretical Atomic and Molecular Physics) website <http://itamp.harvard.edu/>.
6. Carlos Villarreal, "Casimir Forces in Non-Homogeneous Planar and Spherical Systems," presented at the symposium Casimir Forces: Recent Results in Experiment and Theory, Harvard-Cambridge Center for Astrophysics, Harvard University, Cambridge, MA, Nov. 14, 2002. This presentation will be available shortly on line at ITAMP (Institute of Theoretical Atomic and Molecular Physics) website <http://itamp.harvard.edu/>.
7. Raúl Esquivel-Sirvent, Carlos Villarreal, and Cecilia Noguez, "Casimir forces between thermally activated nanocomposites," Materials Research Society Symposium Proceedings 703, 99 (2002).

7.3. Presentations

1. "Much Ado about Nothing: The Role of Empty Space in Modern Science," J. Maclay, Illinois Institute of Technology, Dept. of Chemistry, Physics, and Biology, 1999
2. "Much Ado about Nothing: The Role of Empty Space in Modern Science," J. Maclay, University of Wisconsin at Richland Center, Feb. 2000.
3. "Quantum Vacuum Forces in Rectangular Cavities: What are they and how can we use them?," J. Maclay, UNAM, Physics Institute, Mexico City, Feb. 2000.
4. "Quantum Vacuum Forces in Rectangular Cavities: What are they? How can we measure them? Can we make use of them to power rockets?," J. Maclay, Dept. of Chemistry/Physics" University of Alabama, MSC, June 22, 2000.

5. "Measurement of Quantum Vacuum Forces using an Atomic Force Microscope", M. George, L. Sanderson, J. Maclay, J. Hammer, R. Clark, Eleventh International Conference on Scanning Tunneling, Microscopy/Spectroscopy and Related Techniques, Vancouver, Canada July 15, 2001 (National Research Council of Canada).
6. Superlattice-mediated tuning of the Casimir forces, R. Esquivel-Sirvent, C. Villarreal and G.H. Coccoletzi, Pan-American Advanced Studies Institute: Physics and Technology at the Nanometer Scale, San Jose, Costa Rica, June 24th - July 3rd (2001).
7. Casimir forces in Electromagnetically Induced Transparent, Materials., C. Villarreal, F.J. Lopez, and R. Esquivel-Sirvent, Pan-American Advanced Studies Institute: Physics and Technology at the Nanometer Scale, San Jose, Costa Rica, June 24th - July 3rd (2001).
8. Controlling Casimir forces using heterostructures, R. Esquivel-Sirvent, C. Villarreal and G.H. Coccoletzi, V Workshop on Quantum Field Theory Under the Influence of External Conditions, Leipzig, Germany, September 11th-14th (2001)
9. A three dimensional formula for Casimir forces in finite dielectric slabs., C. Villarreal, W.L. Mochan, and R. Esquivel-Sirvent, V Workshop on Quantum Field Theory Under the Influence of External Conditions, Leipzig, Germany, September 11th-14th (2001).
10. Casimir forces between thermally activated nanocomposites., R. Esquivel-Sirvent, C. Villarreal, and C. Noguez, 2001 Materials Research Society Fall Meeting, Boston, USA, November 26th-30th (2001).
11. J. Maclay, J. Hammer, "Vacuum forces in Microcavities," Proceedings of the Seventh International Conference on Squeezed States and Uncertainty Relations (ICSSUR), Boston, MA, June 4-6, 2001.
12. Jordan Maclay, and Carlos Villarreal, " A Model for Casimir Forces in Closed Cavities with Finite Conductivity," presented at the symposium Casimir Forces: Recent Results in Experiment and Theory, Harvard-Cambridge Center for Astrophysics, Harvard University, Cambridge, MA, Nov. 14, 2002.
13. Carlos Villarreal, "Casimir Forces in Non-Homogeneous Planar and Spherical Systems," presented at the symposium Casimir Forces: Recent Results in Experiment and Theory, Harvard-Cambridge Center for Astrophysics, Harvard University, Cambridge, MA, Nov. 14, 2002.

7.4. Articles in Popular Press/Video

1. On Sept. 27, 2001, the Japanese broadcasting company NHK visited our experiment at the University of Alabama. They filmed the fabrication of the cantilevers, the operation of the AFM, and some of the data as shown on the monitor. They filmed an interview with J. Maclay for about 45 minutes. The experiment and discussion will be in the last segment of a 8 part series discussing science in the new millennium, and will

be broadcast in Japan. HNK is also negotiating with European and US companies to show the series, appropriately reedited, in these countries. The vacuum energy segment has been described by the senior staff at NHK as "one of the most interesting segments." NASA will be credited fully with sponsoring the research.

2. Feature Article on our Quantum Vacuum Project; "Energy Unlimited," by Henry Bortman appeared in New Scientist Magazine, pp32-34, 1/22/2000.
3. The article in Science News about the Casimir experiments at Bell Labs: "Force from empty space drives a machine", Feb. 10, 2001, Vol. 159, No. 6, p. 86, describes our effort to measure repulsive Casimir forces, and listed us and NASA Breakthrough Propulsion Physics as a source of additional information, online as <http://www.sciencenews.org/20010210/fob5ref.asp>
4. "Space at Warp Speed" by Mariette DiChristina, Popular Science, pp 46-51, 5/2001

7.5. Important Recent Citations in MEMS Research to our work:

1. H. B. Chan, V. A. Aksyuk, R. N. Kleiman, D. J. Bishop, F. Capasso (at Bell Labs) "Quantum mechanical actuation of microelectromechanical systems by the Casimir force", Science 291:1941 (2001) cited our work in MEMS systems.
2. H. B. Chan, V. A. Aksyuk, R. N. Kleiman, D. J. Bishop, F. Capasso (at Bell Labs), "Nonlinear micromechanical Casimir oscillator," Phys. Rev. Lett., 87, 211801 (2001), measured Casimir force effects in a MEMS oscillatory system originally proposed by M. Serry, D. Walliser, J. Maclay, "The role of the casimir effect in the static deflection and stiction of membrane strips in microelectromechanical systems (MEMS)," Journal of Applied Physics. 84, 5, pp2501-2506(1998)
3. E. Buks and M. Roukes (at Cal Tech), "Stiction, adhesion energy, and the Casimir effect in micromechanical systems," Phy. Rev. B 63, 033402 (2001), presented measurements of adhesion energy based on M. Serry, D. Walliser, J. Maclay, "The role of the Casimir effect in the static deflection and stiction of membrane strips in microelectromechanical systems (MEMS)," Journal of Applied Physics. 84, 5, pp2501-2506(1998).

8. APPENDIX

For lack of space, we have only included articles not yet available in the literature or on the web.

1. Jordan Maclay and Robert L. Forward, "A Gedanken Spacecraft that accelerates by pushing on the vacuum (Dynamic Casimir Effect), submitted for publication to Physics Letters A.
2. Jordan Maclay, and Carlos Villarreal, " A Model for Casimir Forces in Closed Cavities with Finite Conductivity," submitted for publication to Physics Letters A.
3. P. Milonni, and J. Maclay, "Quantized-Field Description of Light in Negative-Index Media," Submitted to Physical Review A.

Addendum to Final Report

Of the three articles cited in the appendix as unpublished, two of them have now been published and are available in the open literature:

1. Milonni, P.W., and Maclay, "Quantized-Field Description of Light in Negative-Index Media," *Optics Communications*, **228** (2003), pp. 161-165.
2. Maclay, J. and Forward, R., "A Gedanken spacecraft that operates using the quantum vacuum (adiabatic Casimir effect)", *Foundations of Physics*, **34** (March, 2004) pp. 477-500.

The third paper is still under review. For completeness, the submitted text for this paper is included in this Appendix.

- Maclay, J. and Villarreal, C., "A Model for Casimir Forces in Closed Cavities with Finite Conductivity", submitted to Physics Letters A.

A model for Casimir Forces in closed cavities with finite conductivity

G. Jordan Maclay*

Quantum Fields LLC, 20918 Wildflower Lane, Richland Center, WI 53581

Carlos Villarreal

*Instituto de Física, Universidad Nacional Autónoma de México, Apartado Postal
20-364, México, 01000, D.F.*

Abstract

We extend previous calculations of the Casimir forces in perfectly conducting rectangular cavities to finite conductivity by including the plasma frequency as an exponential cutoff. As in the case of perfectly conducting cavities, repulsive forces are predicted for cavities with a finite plasma frequency, but the forces are reduced.

Key words: Casimir, force, rectangular, cavity, conductive

1 Introduction

Casimir forces appear whenever the mode distribution of a fluctuating field is modified by imposing boundary conditions. The most well-known example is the case of quantum vacuum fluctuations of the electromagnetic field distorted by the presence of two infinite, parallel, perfectly-conducting plates [1]. The difference in the vacuum radiation pressure in the region inside and outside

* Corresponding author.

Email address: jordanmaclay@quantumfields.com (G. Jordan Maclay).

¹ Presented at "Casimir Forces:Recent Developments in Experiment and Theory", Harvard-Smithsonian Center for Astrophysics, Cambridge, MA, Nov.14, 2002. The support of the NASA Breakthrough Propulsion Program for this research is gratefully acknowledged.

the plates produces an attractive force (per unit area) between them given by:

$$F(a) = -\frac{\pi^2 \hbar c}{240a^4}, \quad (1)$$

where a is the separation between plates. For plates separated a distance $a \sim 10$ nm, the theoretical pressure is roughly 1 atm. Corrections for finite conductivity and surface roughness have been developed for the parallel plate geometry but not for any other configuration[2][3]. The nature of the Casimir force for this very special parallel plate geometry is not, however, representative of the behavior of Casimir forces in more complicated geometries.

In the case of a perfectly conducting rectangular cavity with lengths a , b , and c , the force acting on each pair of the plates forming the cavity changes sign according to the relative magnitude of the sides[4][5][6]. It is possible to have a cavity with a positive force on two sides, a negative force on two sides, and zero force on two sides. The presence of a positive energy density does not imply that the forces are outward. In general, the Casimir force will tend to be attractive for those pairs of plates with the greatest area and repulsive for the others. For a cubic cavity, the force on all faces is repulsive or outward. This behavior is consistent with the fact that the Maxwell stress tensor satisfies the equality $T_{11} + T_{22} + T_{33} = T_{00}$, so that for of a cavity with a given geometry, the pressures in each direction must accommodate their values to take account of the vacuum energy density inside. The calculated elements T_{ii} and T_{00} are averaged over the jk faces and the cavity volume abc , respectively. For the rectangular cavity the traceless nature of the stress-energy tensor and the relationship $\vec{F} \cdot \vec{a} = en$ follow directly from the fact that the forces and energy must be homogeneous functions of the dimensions $a, b,$ and c . [5]. Here \vec{F} is the total force (F_1, F_2, F_3) on three perpendicular sides, en is the total vacuum energy in the cavity, and $\vec{a} = (a, b, c)$.

Since the seminal work of Casimir in 1948, there have been many theoretical investigations into the use of surfaces and cavities to modify and utilize the structure of the quantum vacuum. However, it is only with the advent of novel experimental techniques associated to the development of micro electro-mechanical systems (MEMS), and instruments such as the atomic force microscope (AFM), that the possible technological implications of these forces are being studied in a realistic fashion. Experimental studies of Casimir forces for parallel metallic plates show excellent agreement with the theoretical predictions. In 1997, using an electromechanical system based on a torsion balance, Lamoreaux [7] reported an agreement with theory at the level of 5%. More recent experiments performed by Mohideen with AFMs achieved precision close to 1% [8,9]. In another experiment, a micromachined torsional device was employed to measure the Casimir attraction between a plate and a spherical metallic surface[10].

Different technological implications of the Casimir forces have been considered in a series of recent works. The deflection associated with Casimir forces acting on a thin microfabricated rectangular strip was calculated by Serry *et al.* [11]. According to their results, the strength of these forces is high enough to control the operation of MEMS. Esquivel-Sirvent *et al.* [12] discussed the possibility of tuning the spatial dependence of Casimir forces by building heterostructures of materials with different dielectric properties, such as a superlattice made of thin metal layers and thicker dielectric layers. The metallic layers would provide a strength of about 80% of the ideal Casimir force, while the dielectric layers would contribute with the richness of their dielectric behavior. This kind of structures could be also useful in the building of Casimir micromotors in which part of the energy cycle could be driven by the Casimir interactions. Such a cycle has been proposed by Pinto [13]. Recently the first dynamic structure based on the Casimir effect appeared, a MEMS device which can be used as a sensitive position sensor, consisting of a plate with a linear restoring force that oscillates anharmonically near another plate[14]. This anharmonic Casimir oscillator (ACO) was first proposed in 1995[15]. Possible applications of geometries which incorporate rectangular cavities were considered by Maclay [16].

The theoretical calculations of the Casimir forces and vacuum energy density for perfectly conducting closed cavities with different geometries have been developed in Refs.[17][18][4][5]. In all these calculations, the conductivity is assumed to be perfect at all frequencies, and the corners infinitely sharp. It is known that perfect conductor boundary conditions are unphysical for curved surfaces. For example, for a perfectly conducting curved surface, Deutsch and Candelas have shown that the vacuum stress energy tensor is approximately proportional to the sum of the reciprocals of the two principal radii of curvature and varies inversely as the cube of the distance to the surface[19]. It follows that the total vacuum energy in any compact region that contains part of the ideal curved conducting surface is infinite. The ether cannot store an infinite amount of energy (whether positive or negative) in a compact region, nor could the conductor support the stress. The perfect conductor boundary conditions are pathological, and lead to an infinite physically observable gravitational field[20].

Indeed Barton has shown for optically thin insulators that the present method of discarding the infinities that occur in the computation of the outward Casimir force on a sphere or the outward force on the faces of a cube is not a proper procedure[21][22]. He maintains that within the discarded infinite terms are embedded important physically meaningful terms and that, in fact, when these terms which include the binding energy of the atoms are included, the net forces become attractive rather than repulsive. Similar results may hold for conductors[23]. Hence, experiments on forces in rectangular cavities have assumed a pivotal importance in understanding the computations

of Casimir forces. It should be pointed out that there are important differences in the behavior of a cube or sphere and the geometries employed in an experiment, namely that in an experiment there are two disjoint surfaces which, when the distance between them is very small, approximate a closed surface. In this paper, we will adopt the customary procedures of the force calculation in which infinite terms are discarded but will include the effect of finite conductivity.

In one proposed experiment using an AFM (Atomic Force Microscope), one measures the force on a metallized sphere about 200 μm in diameter on an AFM cantilever as the sphere approaches a gold surface[16]. The gold surface is essentially a grating, an array of long narrow cavities with walls about 50 nm thick. The desired width of the cavities is about 50 to 500 nm, with a depth of 500-1500 nm. We will calculate the force for a gold grating for this proposed geometry.

For the rectangular cavity, the assumption of perfect conductor boundary conditions lead to energy densities that diverge at the corners. Only by integrating the elements of the stress energy tensor over the corresponding face of the cavity or the volume, as appropriate, can a finite value be obtained. For a real metal, the corners are not infinitely sharp, and the electrons are unable to follow the vacuum electromagnetic field at frequencies above the plasma frequency of the metal. For frequencies above the plasma frequency, the zero-point electromagnetic field is not effectively altered by the presence of the metal plates and the boundary conditions for an ideal conductor are not met. Consequently the net contribution to the renormalized stress energy tensor is expected to be small for frequencies above the plasma frequency. In this paper we will investigate the effect of a finite plasma frequency on the predicted forces in rectangular cavities, finding that applying an exponential cutoff eliminates the divergences.

At the present, the effects of finite conductivity have been only investigated rigorously only for the infinite parallel-plate configuration [24][2]. For this geometry Lifshitz developed a formalism that computes the vacuum force per area in terms of integrals over the frequency ω of functions of the dielectric constant $\epsilon(i\omega)$. To compute the integrals, one needs to know the frequency dependence of the complex dielectric constant over a large frequency interval. The final result for the force/area can be approximated to 5% accuracy simply by multiplying the Casimir force Eq.(1) for a perfect conductor: by a correction factor $C(a)$ [3]:

$$C(a) = \frac{1}{1 + \frac{8}{3\pi} \frac{\lambda_p}{a}} \quad (2)$$

where λ_p is the plasma wavelength. For separations less than the plasma wavelength, $C(a)$ goes to zero linearly while for much larger separations, $C \rightarrow 1$. For gold, the plasma wavelength is estimated to be about 136 nm, which

yields values for C of 0.31, 0.64, and 0.82 at separations of 50 nm, 200 nm and 500 nm respectively[29].

For curved surfaces or for a rectangular cavity, the effect of the finite plasma frequency is expected to be more complex since it must effectively eliminate divergences. We will express the renormalized energy for a perfectly conducting cavity as the limit of an integral over frequency. A cut-off is then added as the imaginary part of an exponent. This approach approximates the effects of a finite conductivity by introducing an explicit exponential cut-off for the higher frequencies of the vacuum modes. Physically this takes into account that real metals are good conductors only for frequencies below their plasma frequency ω_p , while for higher frequencies they become transparent, so that for higher frequencies the net vacuum radiation pressure on the walls of the cavity is negligible. It should be clarified that with this approximate procedure, some questions arise. We are not including any characteristic frequency dependence of the permittivity, such as given by the Drude model, a plasma model, or tabulated data. Nor do we consider a wall of finite thickness, as is present experimentally. Does the use of a cutoff produce terms in the vacuum energy that depend on the molecular properties through the cutoff and, if so, how do these terms depend on the geometry? To date only the sphere has been analyzed in some detail, with the result that a geometry independent, cutoff dependent term has been found[25]. Since the energy term is geometry independent, it does not affect the force.

In the following section, we briefly review the calculations leading to the components of the Maxwell stress tensor for closed cavities, and show the extension for a finite plasma frequency. In Section 3, we give the results of computations of the energy density and Casimir forces for different cavity geometries as a function of the cutoff. In Section 4, we discuss these results, and then give a conclusion.

2 Theory

In this section, we extend the formalism presented in reference [4] to determine the vacuum energy momentum tensor of a perfectly conducting rectangular cavity, to the finite conductivity model. We consider a cavity with lengths a_1 , a_2 , and a_3 , and volume $V = a_1 a_2 a_3$. The use of electric and magnetic Hertz potentials, $\mathbf{\Pi}_e$ and $\mathbf{\Pi}_h$ in the analysis of electromagnetic problems involving boundary conditions has proved to be very useful to handle the real degrees of freedoms of the fields. In terms of these potentials, the H-type modes are obtained from $\mathbf{E}_h = \nabla \times \mathbf{\dot{\Pi}}_h$, and $\mathbf{B}_h = \nabla \times \nabla \times \mathbf{\Pi}_h$, while E-type modes are obtained by replacing $\mathbf{E} \rightarrow \mathbf{B}$, and $e \rightarrow h$ in the former relationships. In

absence of sources, the Hertz potentials satisfy homogeneous wave equations

$$(\nabla^2 - \partial_0^2) \mathbf{\Pi}_{e,h} = 0, \quad (3)$$

where $\nabla^2 = \partial_1^2 + \partial_2^2 + \partial_3^2$, and $\partial_0^2 = c^{-2}\partial_t^2$. In the study of cavities with a rectangular geometry it is convenient to single out some specific direction, *v.gr.*, \mathbf{e}_3 , and write the Hertz potentials as $\mathbf{\Pi}_h = \Psi\mathbf{e}_3$, and $\mathbf{\Pi}_e = \Phi\mathbf{e}_3$, where Ψ and Φ are scalar functions satisfying also the wave equation and appropriate boundary conditions. In these terms, the electric and magnetic fields are expressed in the form

$$\mathbf{E}(x) = (\partial_0\partial_2\Psi + \partial_1\partial_2\Phi, -\partial_0\partial_1\Psi + \partial_2\partial_3\Phi, -\nabla_{\perp}^2\Phi) \quad (4)$$

$$\mathbf{B}(x) = (-\partial_0\partial_2\Phi + \partial_1\partial_2\Psi, \partial_0\partial_1\Phi + \partial_2\partial_3\Psi, -\nabla_{\perp}^2\Psi), \quad (5)$$

with $\nabla_{\perp}^2 = \partial_1^2 + \partial_2^2$. In the case of perfectly conducting cavities, the usual electromagnetic boundary conditions are fulfilled if the potential Φ satisfies Dirichlet boundary conditions on the walls parallel to the \mathbf{e}_3 direction, and Neumann boundary conditions on the walls perpendicular to \mathbf{e}_3 . The converse holds for the potential Ψ , so that the scalar Hertz potentials may be written as follows:

$$\Phi_{n_1n_2n_3} = A_{n_1n_2n_3} \sin\left(\frac{n_1\pi x_1}{a_1}\right) \sin\left(\frac{n_2\pi x_2}{a_2}\right) \cos\left(\frac{n_3\pi x_3}{a_3}\right) e^{(-i\omega_{n_1n_2n_3}t)}, \quad (6)$$

$$\Psi_{n_1n_2n_3} = B_{n_1n_2n_3} \cos\left(\frac{n_1\pi x_1}{a_1}\right) \cos\left(\frac{n_2\pi x_2}{a_2}\right) \sin\left(\frac{n_3\pi x_3}{a_3}\right) e^{(-i\omega_{n_1n_2n_3}t)}, \quad (7)$$

where $\omega_{n_1n_2n_3}^2 = (n_1\pi/a_1)^2 + (n_2\pi/a_2)^2 + (n_3\pi/a_3)^2$, and the normalization coefficients are given by $|A_{n_1n_2n_3}|^2 = |B_{n_1n_2n_3}|^2 = \epsilon_{n_10}\epsilon_{n_20}\epsilon_{n_30}/2V\omega_{n_1n_2n_3}$, where $\epsilon_{n_i0} = 1$ if $n_i = 0$ and $\epsilon_{n_i0} = 2$, otherwise.

The Hertz potentials can be quantized by performing an expansion in terms of creation and annihilation operators

$$\hat{\Phi} = \sum_{n_1,n_2,n_3} (\hat{a}_{n_1n_2n_3} \Phi_{n_1n_2n_3} + \hat{a}_{n_1n_2n_3}^{\dagger} \Phi_{n_1n_2n_3}^*) \quad (8)$$

$$\hat{\Psi} = \sum_{n_1,n_2,n_3} (\hat{b}_{n_1n_2n_3} \Psi_{n_1n_2n_3} + \hat{b}_{n_1n_2n_3}^{\dagger} \Psi_{n_1n_2n_3}^*) \quad (9)$$

satisfying usual commutation relations $[\hat{a}_{n_1n_2n_3}, \hat{a}_{n'_1n'_2n'_3}^{\dagger}] = \delta_{n_1n'_1} \delta_{n_2n'_2} \delta_{n_3n'_3} = [\hat{b}_{n_1n_2n_3}, \hat{b}_{n'_1n'_2n'_3}^{\dagger}]$. By substituting these expansions into Eqs.(3) and (4), we may evaluate the vacuum expectation values of the quantum electromagnetic correlations $\langle 0|E_i(x)E_j(x')|0 \rangle$, $\langle 0|B_i(x)B_j(x')|0 \rangle$, and $\langle 0|E_i(x)B_j(x')|0 \rangle$, whose explicit forms are given in Ref.[4]. This procedure lets us evaluate in turn the mean energy density, and the components of the Maxwell stress tensor:

$$\varepsilon(x, x') = \lim_{x \rightarrow x'} \frac{1}{2} (\langle 0|\mathbf{E}(x) \cdot \mathbf{E}(x')|0 \rangle + \langle 0|\mathbf{B}(x) \cdot \mathbf{B}(x')|0 \rangle) \quad (10)$$

$$T_{ij}(x, x') = \lim_{x \rightarrow x'} \frac{1}{2} \langle 0 | E_i(x) E_j(x') + B_i(x) B_j(x') | 0 \rangle - \frac{1}{2} \delta_{ij} \langle 0 | \mathbf{E}(x) \cdot \mathbf{E}(x') + \mathbf{B}(x) \cdot \mathbf{B}(x') | 0 \rangle. \quad (11)$$

The frequency spectrum of ε and T_{ij} may be obtained by computing a Fourier transform with respect to a finite time interval $t - t' \rightarrow \sigma$ and taking the limit $\mathbf{x} \rightarrow \mathbf{x}'$:

$$\varepsilon(\omega, x) = \lim_{\mathbf{x} \rightarrow \mathbf{x}'} \frac{1}{2\pi} \int d\sigma \varepsilon(x, x') e^{-i\omega\sigma} \quad (12)$$

Integrating over the volume of the cavity, we obtain the energy density:

$$\begin{aligned} \varepsilon(\omega) &= \frac{\hbar}{2\pi^2} \omega^2 \sum_{m_1, m_2, m_3} \frac{\sin(\omega u_{m_1 m_2 m_3})}{u_{m_1 m_2 m_3}} \\ &\quad - \frac{\hbar}{4\pi} \omega \sum_{j=1}^3 \frac{a_j}{V} \sum_{m_j} \cos(2m_j a_j \omega) \end{aligned} \quad (13)$$

where $u_{m_1 m_2 m_3} = [(2a_1 m_1)^2 + (2a_2 m_2)^2 + (2a_3 m_3)^2]^{1/2}$. Similarly the T_{33} component of the Maxwell stress tensor integrated over the area transverse to the direction \mathbf{e}_3 is

$$\begin{aligned} p_3(\omega) &= \frac{\hbar}{2\pi^2} \sum_{m_1, m_2, m_3} \left(\frac{\omega^3 u_{00m_3}}{u_{m_1 m_2 m_3}^2} j_2(\omega u_{m_1 m_2 m_3}) - \frac{\omega^2}{u_{m_1, m_2, m_3}} j_1(\omega u_{m_1 m_2 m_3}) \right) \\ &\quad - \frac{\hbar a_3}{4\pi} \sum_{m_3} \left(\omega j_0(\omega u_{00m_3}) - \frac{d^2}{d\omega^2} [\omega j_0(\omega u_{00m_3})] \right), \end{aligned} \quad (14)$$

where j_n are standard spherical Bessel functions, and similar expressions hold for p_1 and p_2 .

In order to obtain measurable quantities the Casimir energies and forces must be renormalized by subtracting the corresponding quantities associated with a very large cavity configuration, which in our problem is obtained from the limit $a_1, a_2, a_3 \rightarrow \infty$. This is equivalent to discarding the zero-mode terms $m_1 = m_2 = m_3 = 0$ in the triple summations and the terms with $m_i = 0$ in the single summations of Eqs.13 and 14. It is possible to show that these discarded terms provide the mode density $\rho_d(\omega)$ associated with large cavities. In particular, dividing the energy density by $\hbar\omega/2$ we obtain

$$\rho_d(\omega) = \frac{1}{\pi^2} \omega^2 - \frac{1}{2\pi V} \sum_{j=1}^3 a_j, \quad (15)$$

which corresponds to Weyl's asymptotic expression for the mode density of a large rectangular cavity. In the following, we will indicate we have discarded

the divergent zero-mode terms by use of an apostrophe in the summations or on renormalized quantities.

The energy per unit volume ε and force per unit area p_i may be obtained by taking the inverse Fourier transform of Eqs.13 and 14 after the divergences are removed:

$$\varepsilon = \int d\omega \varepsilon'(\omega) e^{i\omega\sigma} \quad (16)$$

. In the case of perfectly conducting finite cavities all frequencies up to infinity contribute and the integrals may be regularized by taking the inverse Fourier transform with respect to $\sigma = t - t'$, and letting $\sigma \rightarrow 0$ (for details see [4]). In the case of rectangular cavities the final results are independent of σ as $\sigma \rightarrow 0$.

However, in the case of more realistic conducting materials, their finite conductivity implies that they are good conductors only for frequencies up to the plasma frequency, while for higher frequencies the material becomes transparent. Such behavior may be taken into account in an approximate way by adding an imaginary component to σ giving $\sigma = t - t' + i\pi/\omega_p$. This yields an exponential cutoff function $f(\omega) = \exp(-\pi\omega/\omega_p)$. This approximation should be reasonable for materials such as gold which show an approximately flat reflectance $R(\omega) \approx 1$ up to ω_p , followed by a sharp decrease for higher frequencies. By introducing the plasma wavelength $\lambda_p = 2\pi c/\omega_p$, the cutoff may be alternatively expressed in terms of the skin depth $\delta = \lambda_p/2\pi$. For a good conductors, such as gold, the plasma frequency $\omega_p \sim 1.5 \times 10^{16}$ Hz, so that the typical skin depth is $\delta \sim .02 \mu\text{m}$. The typical sizes of cavities considered in our study should be greater than 20 nanometers in order that this approximation remain valid.

Introducing the cutoff in Eq.(16) and performing the frequency integration gives the energy density:

$$\begin{aligned} \varepsilon = & -\frac{\hbar c}{16\pi^2} \sum'_{m_1, m_2, m_3} \frac{(a_1 m_1)^2 + (a_2 m_2)^2 + (a_3 m_3)^2 - 3(\lambda_p/4\pi)^2}{((a_1 m_1)^2 + (a_2 m_2)^2 + (a_3 m_3)^2 + (\lambda_p/4\pi)^2)^3} \\ & + \frac{\hbar c}{16\pi} \sum_{j=1}^3 \frac{a_j}{V} \sum'_{m_j} \frac{(a_j m_j)^2 - (\lambda_p/4\pi)^2}{((a_j m_j)^2 + (\lambda_p/4\pi)^2)^2}. \end{aligned} \quad (17)$$

By integrating Eq.(14) the final expression for the force/area p_i is obtained

$$\begin{aligned} p_i = -\varepsilon - & \frac{\hbar c}{16\pi^2} \sum'_{m_1, m_2, m_3} \frac{6(a_i m_i)^2 [(a_1 m_1)^2 + (a_2 m_2)^2 + (a_3 m_3)^2 - 3(\lambda_p/4\pi)^2]}{((a_1 m_1)^2 + (a_2 m_2)^2 + (a_3 m_3)^2 + (\lambda_p/4\pi)^2)^4} \\ & + \frac{\hbar c}{4\pi} \sum_{r=1}^3 \frac{a_r}{V} \sum'_{n_r} \frac{(a_r n_r)^2 - (\lambda_p/4\pi)^2}{((a_r n_r)^2 + (\lambda_p/4\pi)^2)^2}. \end{aligned} \quad (18)$$

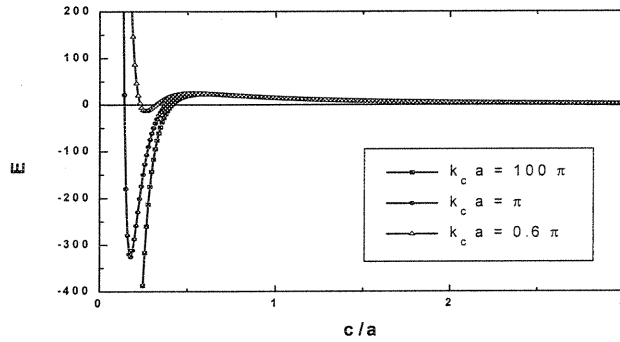


Fig. 1. The dimensionless energy density $E = \varepsilon(16\pi^2 a^4 / \hbar c_0)$ for a cavity with $a=b$ as a function of c/a , plotted for three values of the dimensionless cutoff parameter $k_c a = 2\pi a / \lambda_p = 100\pi, \pi,$ and 0.6π . For $0.4 < c/a < 3$, the energy density is positive for all values of $k_c a$. For $c/a < 0.2$, the geometry is approximately the usual parallel plate geometry and we expect a negative energy density.

The expression for the force/area p_i can also be obtained by equating the virtual work performed by the Casimir force with the virtual change of the vacuum electromagnetic energy of the cavity:

$$p_i(a_1, a_2, a_3) = -\frac{\partial}{\partial a_i} (a_i \varepsilon(a_1, a_2, a_3)). \quad (19)$$

The final results for $\varepsilon(a_1, a_2, a_3)$ and $p_i(a_1, a_2, a_3)$ agree with corresponding results for a perfect conductor [18,4] in the limit $\lambda_p \rightarrow 0$.

In the following section we present the numerical results for different cavity configurations with different plasma frequencies.

3 Results

We computed the dimensionless energy density $E = 16\pi^2 \varepsilon a^4 / \hbar c_0$ and the dimensionless pressure $P_z = 16\pi^2 p_z a^4 / \hbar c_0$ in the z direction for a cavity with dimensions $a \times b \times c$ as a function of c/a for different values of the the ratio b/a and the dimensionless cutoff parameter $k_c a = a\omega_p / c_0 = 2\pi(a/\lambda_p)$, where ω_c is the plasma frequency and λ_p is the plasma wavelength.

Figures 1 and 2 show E and P_z , respectively, versus c/a for a cavity with $b = a$, for $k_c a = 0.6\pi, \pi,$ and 100π . The curves in Figure 1 can be viewed as showing the effect of the magnitude of $k_c = \omega_c c_0$ on the value of the renormalized vacuum energy density e for a cavity of fixed dimension a . The curve with $k_c a = 100\pi$ corresponds to a very conductive cavity, with plasma wavelength $\lambda_c = a/50$. Indeed this curve is identical to the curve for an

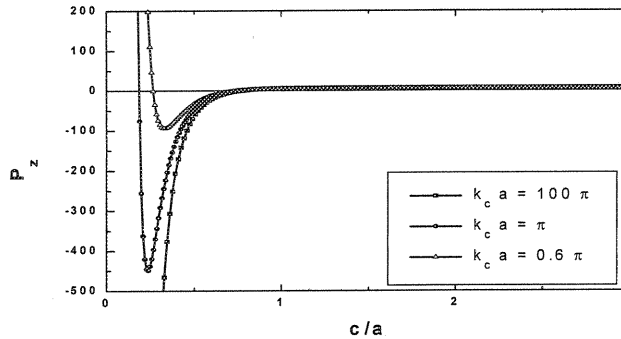


Fig. 2. The dimensionless pressure $P_z = 16\pi^2 p_z a^4 / \hbar c_0$ in the z -direction as a function of c/a , corresponding to the cavity in Figure 1, with $a=b$, for $k_c a = 2\pi a / \lambda_p = 100\pi, \pi, \text{ and } 0.6\pi$. A positive force is repulsive.

infinite plasma frequency for the region plotted. For $0.4 < c/a < 3$, the energy is positive; for $c/a < \sim 0.4$, the energy drops to zero and then rapidly becomes more negative. The asymptotically infinite negative value of e for small separations corresponds to the usual $1/a^3$ divergence for the energy for the infinite parallel plate configuration. The intermediate curve for $k_c a = \pi$ corresponds to a plasma wavelength that is $2a$. In this case, the energy density e follows the curve for the previous case until e drops to zero. In the interval, $0.15 < c/a < 0.4$, the energy corresponding to the lower plasma frequency is not as negative as that corresponding to the ideal conductivity case. At about $c/a \sim 0.1$, the curve for e corresponding to $k_c a = \pi$ reaches a minimum, and begins to increase asymptotically. This energy minimum in e is a distinct feature associated with a low plasma frequency and is probably a computational artifact as discussed in Section 4.

Figure 2 shows the dimensionless pressure P_z in the z -direction corresponding to the same configuration $a = b$ and conditions $k_c a = 0.6\pi, \pi, \text{ and } 100\pi$ as in Figure 1. For all three cutoffs, the pressure p_z has the same slightly positive values for $0.7 < c/a$. For $c/a < 0.7$, the pressure becomes more negative, dropping more quickly the larger the plasma frequency. The curve for $k_c a = 100\pi$ is the same as the infinite conductivity curve for the region plotted. The negative or attractive force for very small separations corresponds to the parallel plate geometry case. The curve for $k_c a = 0.6\pi, \pi$ reach a minimum negative value and begin to increase rapidly. This behavior of P_z is a distinct feature that follows from the finite plasma frequency, and probably signals a breakdown in the approximations.

Figures 3 and 4 show the same cases as Figures 1 and 2, but with a magnified scale for the ordinate axis. Figures 5 and 6 show E and P_z , respectively, for $b = 10a$, for $k_c a = 0.6\pi, \pi, \text{ and } 100\pi$. show the corresponding results for $b = 10a$.

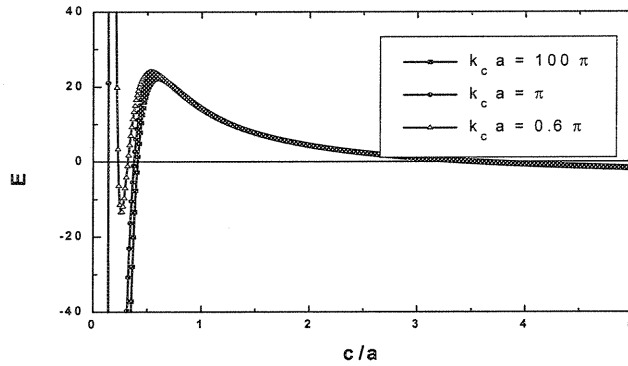


Fig. 3. A magnified view of the energy (as shown in Figure 1) as a function of c/a for a cavity with $a = b$, for three values of the plasma frequency. $k_c a = 2\pi a/\lambda_p = 100\pi, \pi,$ and 0.6π .

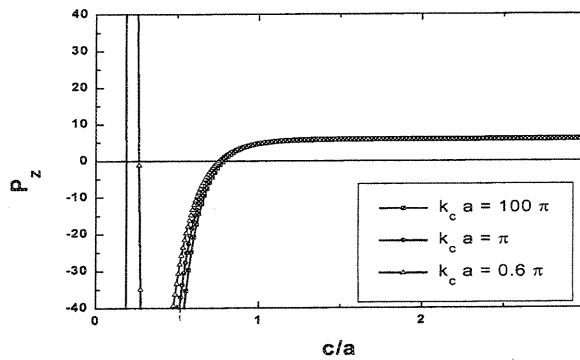


Fig. 4. A magnified view of the pressure P_z (as shown in Figure 2) as a function of c/a for a cavity with $a = b$, for $k_c a = 100\pi, \pi,$ and 0.6π . The pressure is repulsive for $c/a > 0.8$ independent of different values of the plasma frequency cutoff.

Figures 7 and 8 show the effect of a finite plasma wavelength on the total force F_z in the z direction as a function of c for a gold cavity that has $b = 120$ nm, and $b = 40$ nm respectively, both cavities with $a = 100$ μm .

4 Discussion

For all geometries the curves for E and P_z follow a general pattern. For large values of $c/a (> \sim 2.5)$, P_z is asymptotically a repulsive force. The predicted asymptotic behavior is the same for all plasma frequencies, therefore this asymptotic prediction appears to be independent of the conductivity of

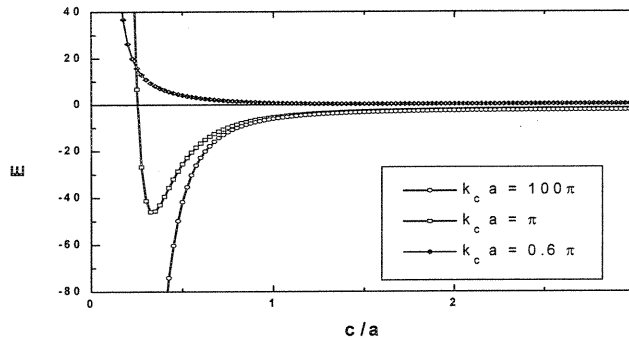


Fig. 5. The vacuum energy for a cavity with $b = 10a$ plotted as a function of c/a for $k_c a = 100\pi$, π , and 0.6π . In general, the more conductive the cavity, the larger the vacuum energy.

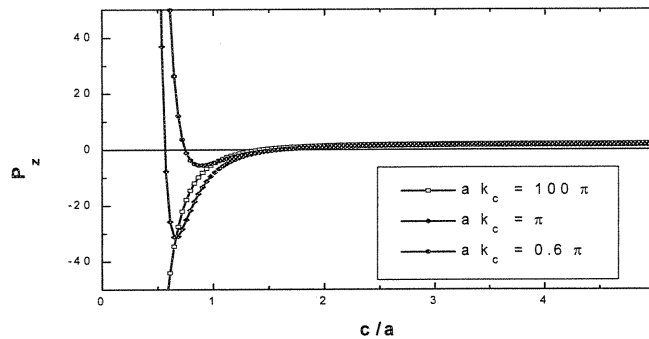


Fig. 6. The pressure corresponding to the vacuum energy in Figure 7, for a cavity with $b=10a$, shown as a function of c/a for $k_c a = 100\pi$, π , and 0.6π . The pressure is repulsive for $c/a > 2$ independent of plasma frequency.

the material. This result suggests that longer wavelength fluctuations seem to be associated with repulsive forces. Conversely, for small values of c/a , the force P_z becomes strongly attractive and the energy density becomes negative as the geometry begins to approximate the usual parallel plate configuration. The value of c/a at which the force P_z changes sign is approximately equal to $\{\text{the smaller of } a \text{ and } b\}/c$. The higher the plasma frequency, the greater the conductivity, and the larger the value of c/a at which the force P_z becomes negative.

For very small values of c/a , and low plasma frequencies ($k_c = \pi, 0.7\pi$), the energy reaches a minimum negative value, and then increases. The corresponding force becomes strongly repulsive. It would be very interesting (and unexpected) if this behavior was observed. It would suggest the existence of stable configurations for cavities. Indeed, Ford has suggested that there may

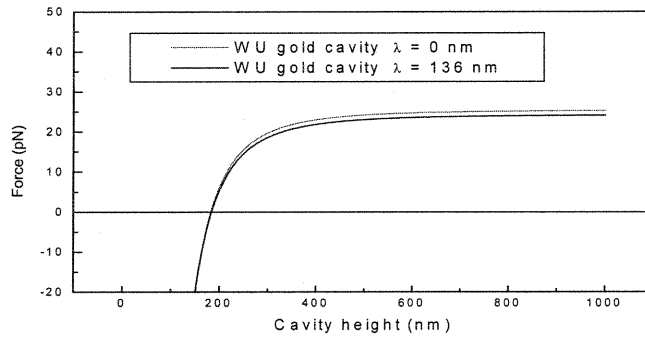


Fig. 7. The total force of the face of a cavity that is 120 nm wide by 100 μm long as a function of the depth of the cavity. The force is given for a perfect conductor ($\lambda_p = 0$, upper curve) and for gold ($\lambda_p = 136$ nm, lower curve).

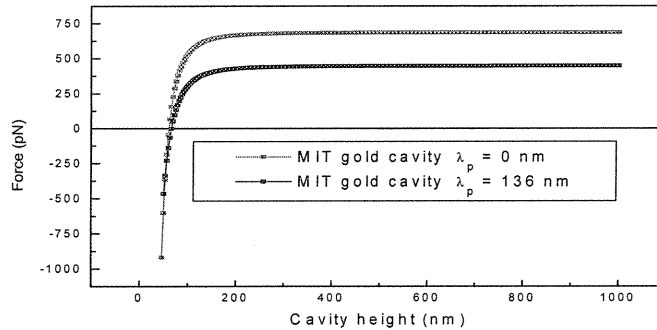


Fig. 8. The total force of the face of a cavity that is 40 nm wide by 100 μm long as a function of the depth of the cavity. The force is given for a perfect conductor ($\lambda_p = 0$, upper curve) and for gold ($\lambda_p = 136$ nm, lower curve).

be stable locations for a polarizable particle in front of a real metal plate [35]. In his analysis, these stable locations arise from the Drude dielectric function considered and do not appear for a perfect conductor. In the rectangular cavity geometries examined here, the repulsive forces occur when one or more dimensions are typically of the order of a tenth of the plasma wavelength. This means that wavelengths of the order of the smallest cavity dimension (and perhaps the next smallest also) are being excluded from the computation. In general, wavelengths of the order of the dimensions give the dominant contribution to the energy and force. Hence in these cases, the approximation of using a plasma frequency cutoff to obtain the force for a imperfect conductor is probably not accurate, and the repulsive forces are a computational artifact. On the other hand, in the regions in which the energy and force curves show similar a behavior for all values of the cutoff parameters, all dimensions are of the order of the plasma wavelength or greater, and the

resulting computations are expected to more accurate.

Figures 7 and 8 show the total force F_z on top face of a rectangular cavity as a function of the cavity depth for a 120 nm wide x 100 μm long cavity and a 40 nm wide x 100 μm long cavity, with plasma frequency $\lambda_p = 136 \text{ nm}$ ($\omega_p \sim 1.4 \times 10^{16} \text{ s}^{-1}$) corresponding to gold. The skindepth is $\delta \sim 22 \text{ nm}$. Cavities should have dimensions of the order of 50 nm or more for our approximations to remain valid and the cavity walls should be at least 35 nm thick [2]. The finite conductivity reduces the repulsive force by about a third. In principle, the predicted forces are large enough to be measurable, however, in an experiment in which a sphere on an AFM cantilever is suspended closely over a cavity, there are significant additional effects due to the finite thickness of the cavity walls and the fact that the cavity is not truly closed[16].

5 Conclusion

The Casimir force in a rectangular cavity made of a material with finite conductivity has been calculated approximately by incorporating a finite plasma frequency as a cut off. Based on the results, it appears that cavities made of materials with finite conductivity would generally be expected to behave in a manner similar to ideal cavities made of a perfect conductor, except that the Casimir forces will be reduced. If repulsive forces are indeed measurable in perfectly conducting cavities, then reduced repulsive forces should also be measurable in cavities made of real materials. A more accurate computation, in which includes a realistic dielectric function and binding energies might reveal other interesting features not apparent in the simplified one parameter approach taken in this calculation.

References

- [1] H. B. G. Casimir, Proc. Kon. Ned. Akad. Wet. **51**, 793 (1948); G. Plunien, B. Müller and W. Greiner, Phys. Rep. **134** (1986) 87.
- [2] G. L. Klimchitskaya, A. Roy, U. Mohideen, and V. M. Mostepanenko, Phys. Rev A **60** (1999) 3487.
- [3] A. Lambrecht and S. Reynaud, Phys. Rev. Lett., **84** (2000) 5672.
- [4] S Hacyan, R Jauregui, and C Villarreal, Phys. Rev. A, Vol. **47** (1993) 4204
- [5] G. Jordan Maclay, Phys. Rev. A **61** (2000) 052110.
- [6] V. Mostepanenko and N. Trunov, *The Casimir Effect and its Applications*, Clarendon Press, Oxford 1997.

- [7] S. K. Lamoreaux, Phys. Rev. Lett. **78** (1997) 5.
- [8] U. Mohideen and Anushree Roy, Phys. Rev. Lett. **81** (1998) 4549.
- [9] B. W. Harris, F. Chen, and U. Mohideen, Phys. Rev. A **62** (2000) 052109.
- [10] H. B. Chan, V. A. Aksyuk, R. N. Kliman, D. J. Bishop and F. Capasso, Science **291** (2001) 1942.
- [11] F. M. Serry, D. Walliser and G. J. Maclay, J. Appl. Phys. **84** (1998) 2501.
- [12] R. Esquivel-Sirvent, C. Villarreal, G. Cocolletzi, Phys. Rev A **64** (2001) 052108.
- [13] F. Pinto, Phys. Rev. B **60** (1999) 14740.
- [14] H. B. Chan, V. A. Aksyuk, R. N. Kleiman, D. J. Bishop, F. Capasso, Phys. Rev. Lett. **87** (2001) 211801
- [15] M. Serry, D. Walliser, J. Maclay, IEEE-ASME Journal of Microelectromechanical Systems **4** (1995) 193.
- [16] J. Maclay, J. Hammer, *Vacuum forces in microcavities*, Seventh International Conference on Squeezed States and Uncertainty Relations (ICSSUR), Boston, June 2001. Proceedings available at <http://www.physics.umd.edu/robot/>; J. Maclay, *A design manual for micromachines using Casimir forces: preliminary considerations*, PROCEEDINGS of STAIF-00 (Space Technology and Applications International Forum-2000, Albuquerque, NM, January, 1999), edited by M.S. El-Genk, AIP Conference Proceedings 354, American Institute of Physics, New York 2000. Published in hardcopy and CD-ROM by AIP.
- [17] J. Ambjorn, and S. Wolfram, Annals of Physics **147** (1983) 1-32 .
- [18] W Lukosz, Physica **56** (1971) 109.
- [19] D. Deutsch and P. Candelas, Phys. Rev. D **20** (1979) 3063.
- [20] B. deWitt in *Physics in the Making*, edited by A Sarlemijn and M. Sparnaay, Elsevier, Amsterdam, 1990.
- [21] G. Barton, J. Phys. A.: Mathematical and General **34** (2001) 4083.
- [22] G. Barton, Int. J. Mod. Phys. A **17** (2002) 767.
- [23] G. Barton, "Casimir effects for a conducting spherical shell: between C₆₀ and the Lamb shift," presented at the workshop Casimir Forces: Recent Developments in Experiment and Theory, Harvard-Smithsonian Center for Astrophysics, Cambridge, MA, November, 2002.
- [24] E. M. Lifshitz, Sov. Phys. JETP **2** (1956) 73.
- [25] P. Candelas, Annals of Physics **143** (1982) 241-295.
- [26] C. Villarreal, Phys. Rev. D **51** (1995) 2959.
- [27] L. S. Brown and G. J. Maclay, Phys. Rev. **184** (1969) 1272.

- [28] T. D. Stowe, K. Yasamura, T.W. Kenny, *et al.*, Appl. Phys. Lett. **71** (1997) 288.
- [29] G. L. Klimchitskaya, U. Mohideen, V. M. Mostepanenko, Phys. Rev. A **61** (2000) 22115.
- [30] W. Chen and H. Ahmed, Appl. Phys. Lett. **63** (1993) 1116.
- [31] E. Buks and M. L. Roukes, Phys. Rev. B **63** (2001) 033402.
- [32] H. Chan, V. Aksyuk, R. Kleiman, D. Bishop, and F. Capasso, Science **291** (2001) 1941.
- [33] H. B. Chan, V. A. Aksyuk, R. N. Kleiman, D. J. Bishop, and F. Capasso, Phys. Rev. Lett. **87** (2001) 211801.
- [34] S. Hacyan, R. Jáuregui, F. Soto, and C. Villarreal, J. Phys. A **23** (1990) 2401.

REPORT DOCUMENTATION PAGE			<i>Form Approved</i> <i>OMB No. 0704-0188</i>	
Public reporting burden for this collection of information is estimated to average 1 hour per response, including the time for reviewing instructions, searching existing data sources, gathering and maintaining the data needed, and completing and reviewing the collection of information. Send comments regarding this burden estimate or any other aspect of this collection of information, including suggestions for reducing this burden, to Washington Headquarters Services, Directorate for Information Operations and Reports, 1215 Jefferson Davis Highway, Suite 1204, Arlington, VA 22202-4302, and to the Office of Management and Budget, Paperwork Reduction Project (0704-0188), Washington, DC 20503.				
1. AGENCY USE ONLY (Leave blank)		2. REPORT DATE October 2004	3. REPORT TYPE AND DATES COVERED Final Contractor Report	
4. TITLE AND SUBTITLE Study of Vacuum Energy Physics for Breakthrough Propulsion			5. FUNDING NUMBERS WBS-22-62-949-10-01 NAS3-00093	
6. AUTHOR(S) G. Jordan Maclay, Jay Hammer, Rod Clark, Michael George, Yeong Kim, and Asit Kir				
7. PERFORMING ORGANIZATION NAME(S) AND ADDRESS(ES) Quantum Fields LLC 20876 Wildflower Lane Richland Center, Wisconsin 53581			8. PERFORMING ORGANIZATION REPORT NUMBER E-14771	
9. SPONSORING/MONITORING AGENCY NAME(S) AND ADDRESS(ES) National Aeronautics and Space Administration Washington, DC 20546-0001			10. SPONSORING/MONITORING AGENCY REPORT NUMBER NASA CR-2004-213311	
11. SUPPLEMENTARY NOTES G. Jordan Maclay, Quantum Fields LLC, 20876 Wildflower Lane, Richland Center, Wisconsin 53581; Jay Hammer and Rod Clark, MEMS Optical, Inc., 205 Import Circle, Huntsville, Alabama 35806; and Michael George, Yeong Kim, and Asit Kir, University of Alabama, 301 Sparkman Drive, Huntsville, Alabama 35805. Project Manager, Marc G. Millis, Turbomachinery and Propulsion Systems Division, NASA Glenn Research Center, organization code 5870, 216-977-9535.				
12a. DISTRIBUTION/AVAILABILITY STATEMENT Unclassified - Unlimited Subject Categories: 20 and 70 Available electronically at http://gltrs.grc.nasa.gov This publication is available from the NASA Center for AeroSpace Information, 301-621-0390.			12b. DISTRIBUTION CODE	
13. ABSTRACT (Maximum 200 words) This report summarizes the accomplishments during a three year research project to investigate the use of surfaces, particularly in microelectromechanical systems (MEMS), to exploit quantum vacuum forces. During this project, we developed AFM instrumentation to repeatably measure Casimir forces in the nanoNewton range at 10^{-6} torr, designed an experiment to measure attractive and repulsive quantum vacuum forces, developed a QED based theory of Casimir forces that includes non-ideal material properties for rectangular cavities and for multilayer slabs, developed theoretical models for a variety of microdevices utilizing vacuum forces, applied vacuum physics to a gedanken spacecraft, and investigated a new material with a negative index of refraction.				
14. SUBJECT TERMS Interstellar travel; Spacecraft propulsion; Physics; Gravitation; Antigravity			15. NUMBER OF PAGES 54	
			16. PRICE CODE	
17. SECURITY CLASSIFICATION OF REPORT Unclassified	18. SECURITY CLASSIFICATION OF THIS PAGE Unclassified	19. SECURITY CLASSIFICATION OF ABSTRACT Unclassified	20. LIMITATION OF ABSTRACT	

